

**UNCLASSIFIED**

**AD 406 088**

**DEFENSE DOCUMENTATION CENTER**

**FOR**

**SCIENTIFIC AND TECHNICAL INFORMATION**

**CAMERON STATION, ALEXANDRIA, VIRGINIA**



**UNCLASSIFIED**

**NOTICE:** When government or other drawings, specifications or other data are used for any purpose other than in connection with a definitely related government procurement operation, the U. S. Government thereby incurs no responsibility, nor any obligation whatsoever; and the fact that the Government may have formulated, furnished, or in any way supplied the said drawings, specifications, or other data is not to be regarded by implication or otherwise as in any manner licensing the holder or any other person or corporation, or conveying any rights or permission to manufacture, use or sell any patented invention that may in any way be related thereto.

SUMMARY REPORT

INFRARED PHOTOCONDUCTORS

Contract Nonr-2225(00)

December 31, 1962

for

Office of Naval Research  
DEPARTMENT OF THE NAVY  
Washington, D. C.

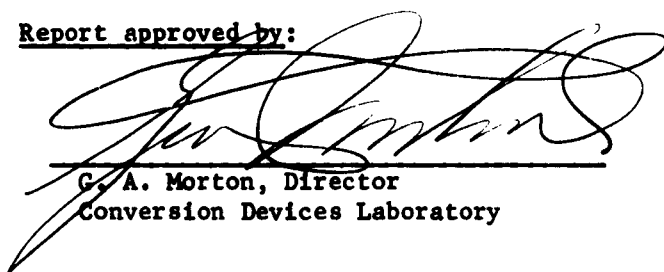
Work done by:

M. L. Schultz, Project Engineer  
W. E. Harty  
C. D. Rowley

Report prepared by:

M. L. Schultz

Report approved by:



A large, stylized handwritten signature in black ink, appearing to read 'G. A. Morton', is written over a horizontal line.

G. A. Morton, Director  
Conversion Devices Laboratory

RADIO CORPORATION OF AMERICA  
Conversion Devices Laboratory  
Electron Tube Division  
RCA Laboratories  
Princeton, N. J.

## TABLE OF CONTENTS

	<u>page</u>
OBJECTIVE -----	iii
INTRODUCTION -----	1
PART I	
EXTRINSIC PHOTOCONDUCTORS FOR THE 3-5 MICRON SPECTRAL REGION	
I. Introduction -----	2
II. Gold Doped Germanium-Silicon Alloys -----	6
A. Relative Spectral Response Characteristics -----	6
B. Magnitude of Photocurrent -----	9
C. Detectivities -----	11
III. Cobalt <sup>II</sup> Doped Germanium -----	14
IV. Nickel Doped Germanium -----	21
V. Materials Preparation -----	24
A. Gold Doped Germanium-Silicon Alloy -----	24
B. Nickel Doped Germanium -----	24
C. Cobalt Doped Germanium -----	25
PART II	
COMPENSATED DONOR PHOTOCONDUCTORS	
I. Introduction -----	26
II. Materials Preparation -----	31
A. Gold Doped Germanium -----	31
B. Cobalt Doped Germanium -----	31
III. Model of Compensated Donor Photoconductor -----	33
IV. Cobalt <sup>I</sup> Doped Germanium -----	41
A. Energy Levels -----	41
B. Black Body Photoconductive Response -----	41
C. Spectral Response Characteristics -----	43
D. Temperature Dependence of Photocurrent -----	46
E. Relative Quantum Yield -----	48
V. Gold <sup>I</sup> Doped Germanium -----	50
A. Temperature Dependence of Resistivity -----	50
B. Black Body Photoconductive Response -----	53
C. Spectral Response Characteristics -----	54
D. Temperature Dependence of Photocurrent -----	54

## OBJECTIVE

To investigate extrinsic germanium photoconductors activated with such impurities as cobalt or gold where a donor level near the valence band is compensated with an acceptor. Under these circumstances, the donor level becomes a pseudo-acceptor level and can serve as the activator for infrared photoconductivity. Under certain operating conditions, such activator centers should have much smaller capture cross-sections than normal acceptor centers, which should be reflected in greater responsivity. Other anomalous effects might also be expected.

The efficacy of extrinsic germanium as a relatively short wavelength ( $5 \mu$ ) infrared photoconductor is also to be explored. Nickel as an impurity in germanium is an acceptor with an ionization energy of about 0.23 electron volts. Material with this activator will be prepared and tested. Two other short wavelength photoconductors are also of interest and will be investigated. These are cobalt in germanium and gold in germanium-silicon alloy.

## INTRODUCTION

Two lines of research on extrinsic germanium photoconductors are described in this report. Part I deals with an investigation of photoconductors designed to function in the 3 to 5 micron region. For this, germanium-silicon alloys activated with Au<sup>II</sup> and germanium activated with Co<sup>II</sup> or Ni<sup>I</sup> were studied. Germanium activated with nickel appeared to be the best solution, although its peak response is somewhat below 5  $\mu$ . It is probable that when prepared with optimum compensation, its performance would equal that of the known intrinsic photoconductors. Its stability, uniformity, and ease of preparation might be superior. Part II treats the behavior of photoconductors using compensated donor levels near the valence band as pseudo acceptor activators. The lowest levels of gold (25  $\mu$ ) and cobalt (15  $\mu$ ) were examined. Promising results were obtained, but further work is required to determine whether advantage can be taken of the possible two or three orders of magnitude increase in lifetime (and consequently in photoconductive gain) which should be available.

## PART I

## EXTRINSIC PHOTOCONDUCTORS FOR THE 3-5 MICRON SPECTRAL REGION

I. Introduction

The development of detectors for the infrared spectral region between 2.5 and 5.5 microns is important since useful atmospheric transmission bands and strong emission bands due to water vapor and carbon dioxide fall within this range and since an appreciable fraction of the total radiation from sources of moderate temperatures lies within these limits. The detector materials currently available having long wavelength thresholds in the neighborhood of 5 to 6 microns include indium antimonide, lead selenide, and lead telluride. These are all intrinsic photoconductors. There has been relatively little investigation of the potentialities of extrinsic photoconductors specifically for this wavelength range although there are reasons to expect that properly prepared materials of this type should at least equal in performance the best of the intrinsic detectors. The present report summarizes the results of some preliminary studies of the behavior of short wavelength threshold extrinsic photoconductors.

A semi-empirical relationship between  $D_M^*$ , the detectivity at the peak of the extrinsic response,  $\lambda_{Th}$ , the threshold wavelength defined as the wavelength at which the response is a factor of ten below the peak value, and T, the operating temperature in degrees Kelvin, may be written<sup>1</sup> provided that the detector is operating under generation-recombination noise limited conditions. This relationship is:

$$\log D_M^* = A + B \left( \frac{1}{\lambda_{Th} T} \right) \quad (1)$$

A is characteristic of the particular photoconductor while B contains only fundamental constants. The values of A and B which give the best empirical fit to

---

1. G. A. Morton, M. L. Schultz, and W. E. Harty, RCA Rev. 20, 599(1959).

to data for several extrinsic photoconductors are 6.40 and  $2.56 \times 10^3$  micron degrees, respectively.

If, for the 3 to 5 micron detector, the response at about 5 microns is to be no more than a factor of about two below the peak value, the photoconductive threshold as defined above would have to lie at approximately 6.5 microns. This corresponds to an optical ionization energy of 0.19 ev. The predicted  $D_M^*$  from Eq. (1) corresponding to the above threshold is  $3 \times 10^{11}$  cm watt<sup>-1</sup> sec<sup>-1/2</sup>. when the detector is operated at liquid nitrogen temperature. It should, of course, be kept in mind that if the detector performance is limited by amplifier noise or by other non-fundamental noise sources or if it is limited by background radiation noise, Eq. (1) no longer applies.

Of the known impurities in germanium, those most nearly satisfying the ionization energy requirement for the 3 to 5 micron detector include the lowest lying acceptor levels of cobalt and nickel at 0.25 ev and 0.23 ev above the valence band edge, respectively; the second acceptor level of mercury at 0.23 ev and the donor level of sulfur at 0.18 ev below the conduction band edge. Except for sulfur doped germanium, which is probably difficult to prepare because of the volatility and reactivity of sulfur, these levels are somewhat too deep-lying to provide complete coverage of the 3-5 micron region.

Extrinsic photoconductors having the desired spectral response characteristics can be obtained by taking advantage of the fact that the activation energy of an impurity in germanium-silicon alloys is a function of the alloy composition.<sup>1</sup> Of particular interest for the present application is the lowest lying acceptor level of gold which, in germanium, lies at 0.15 ev above the valence band edge. In an alloy containing about ten atom percent silicon, the activation energy has approximately the desired value. The investigation of

this type of material was commenced under Contract AF33(616)-6249<sup>2</sup> and was continued under the present contract. Initial experiments were carried out with samples gold doped by diffusion. Although the results obtained did demonstrate the dependence of optical ionization energy upon alloy composition, some of the properties of these samples; in particular, the thermal activation energy and the magnitude of the noise, were found to depend strongly upon the presence or absence of traces of oxidizing agents in the ambient atmosphere present during diffusion and upon the low temperature (near 500°C) heat treatment history of the samples. These effects are believed to be due to the presence of oxygen centers similar to those which have been described in the literature for oxygen in germanium or silicon. Under some circumstances, such centers exhibit donor action. Their presence greatly complicates the control of compensation of the gold centers.

In view of this complex behavior, doping from the melt was adopted as the more satisfactory preparation procedure. As appears always to be the case in growing alloy crystals, addition of a donor impurity was necessary to compensate residual shallow acceptor impurities. Investigation of melt doped samples revealed a dependence of the optical ionization energy of the gold level upon degree of compensation as well as upon alloy composition. It proved to be difficult to control the compensation to the precision required to obtain high photoconductive gain. Consequently, the performance of the detectors made from gold doped germanium-silicon alloy was usually limited by the condition that the noise as a function of bias voltage entered the noise breakdown region before the noise from the detector had risen appreciably above the Johnson noise of the load resistor. This limitation is non-fundamental and would be removed if the photoconductive gain could be increased sufficiently.

---

2. K. S. Ling, WADD Technical Report 61-140, Contract AF33(616)-6249, 31 Jan. 1961.

At this point, the investigation of cobalt and of nickel doped germanium was undertaken with the hope that in these materials the control of compensation would be less difficult than in the gold doped alloy system. The very small segregation coefficients of these impurities in germanium dictate diffusion doping to achieve adequately large concentrations. However, their very rapid rates of annealing-out during quenching from the diffusion temperature plus the fact that low-lying acceptor states (probably due to vacancies) are produced when annealing occurs give rise to complications with these also in the control of compensation. Within the limitations of time imposed on this work, it was not possible to achieve optimum compensation. It has been possible, however, in spite of these deficiencies to achieve peak detectivities for cobalt and nickel doped germanium and gold doped germanium-silicon alloy in excess of  $10^{10}$  cm watt<sup>-1</sup> sec<sup>-1/2</sup> at operating temperatures of 77°K or higher. A sufficiently detailed study of the doping of these materials should lead to control of the compensation to an extent such that the performance should be significantly improved.

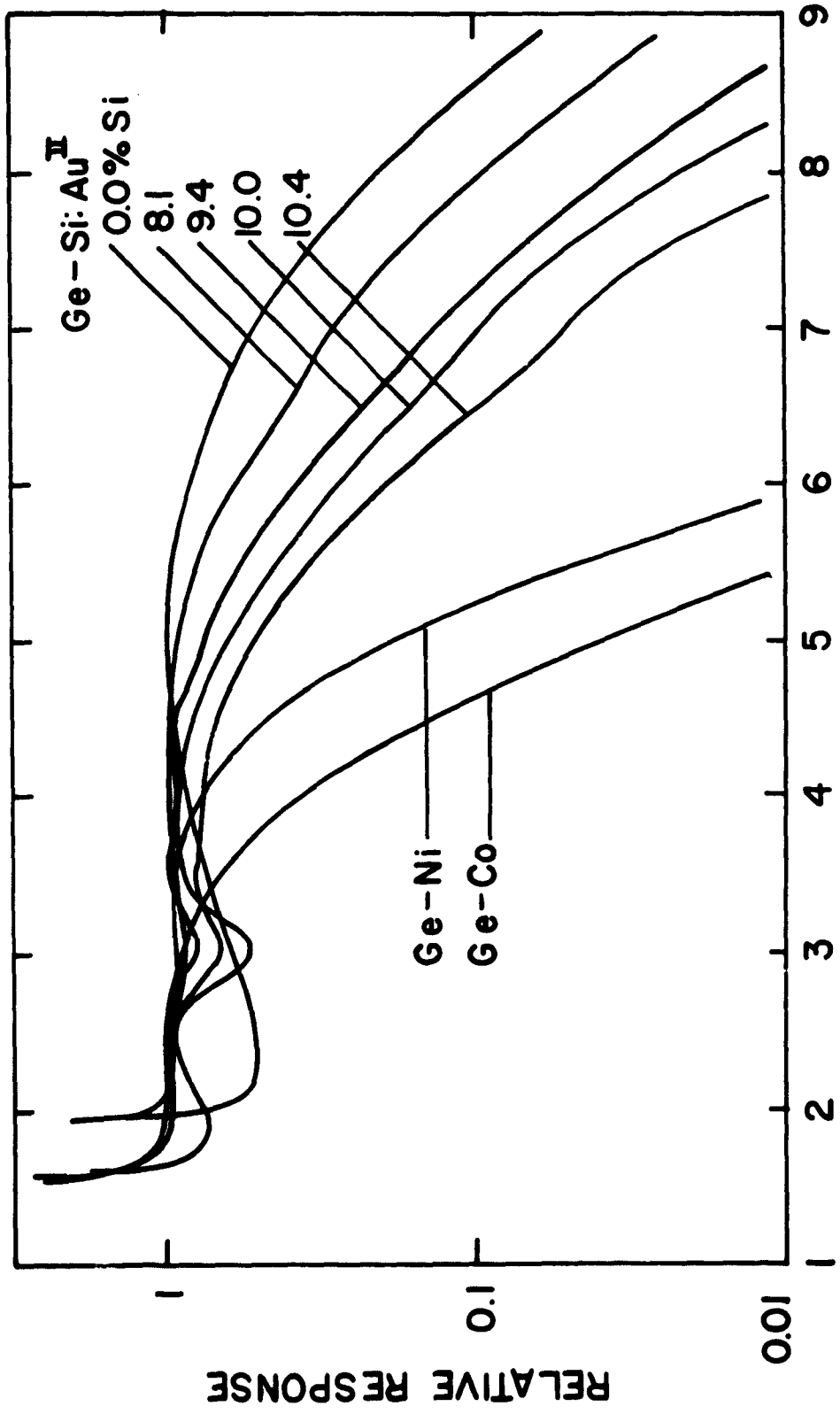
## II. Gold Doped Germanium-Silicon Alloys<sup>3</sup>

### A. Relative Spectral Response Characteristics

A family of spectral response curves, normalized to unity at the peak of the extrinsic response, is shown in Fig. 1. These curves illustrate clearly the shift of the photoconductive threshold to shorter wavelengths with increasing silicon content. Also shown on this figure are relative spectral response curves for nickel and for cobalt doped germanium. Comparison of these with the gold doped alloy curves illustrates the more complete coverage of the 3 to 5 micron region which is attainable with the gold doped alloy photoconductors. The effect of the degree of compensation of the gold level in the alloys is illustrated by the curves of Fig. 2 in which the dependence of threshold upon silicon content is given for crystals 487 and 488. For silicon contents larger than about 6 atom percent, the data for the two crystals indicate a shift of about one micron in the threshold which appears to be due to differences in the degree of compensation in the two crystals. The number beside each point or group of points gives the percentage compensation of the gold level. The threshold shifts to shorter wavelengths with increasing compensation. This effect has previously been noted<sup>1</sup> for zinc doped alloys and is probably a general phenomenon. Its existence gives rise to the hypothesis that an impurity in the alloys must be characterized by a distribution of states in energy rather than by a single level at a sharply defined energy. Such a situation could arise since different impurity atoms will have, in general, different distributions of germanium and silicon atoms in their neighborhood. If such a distribution of levels exists, the lower lying will be compensated first as the donor concentration is increased with the result that photoexcitation of holes can occur only from the deeper lying uncompensated levels of the distribution.

---

3. Some of the results reported in this section were obtained under Contract AF33(616)-6249.



MICRONS  
FIG. I

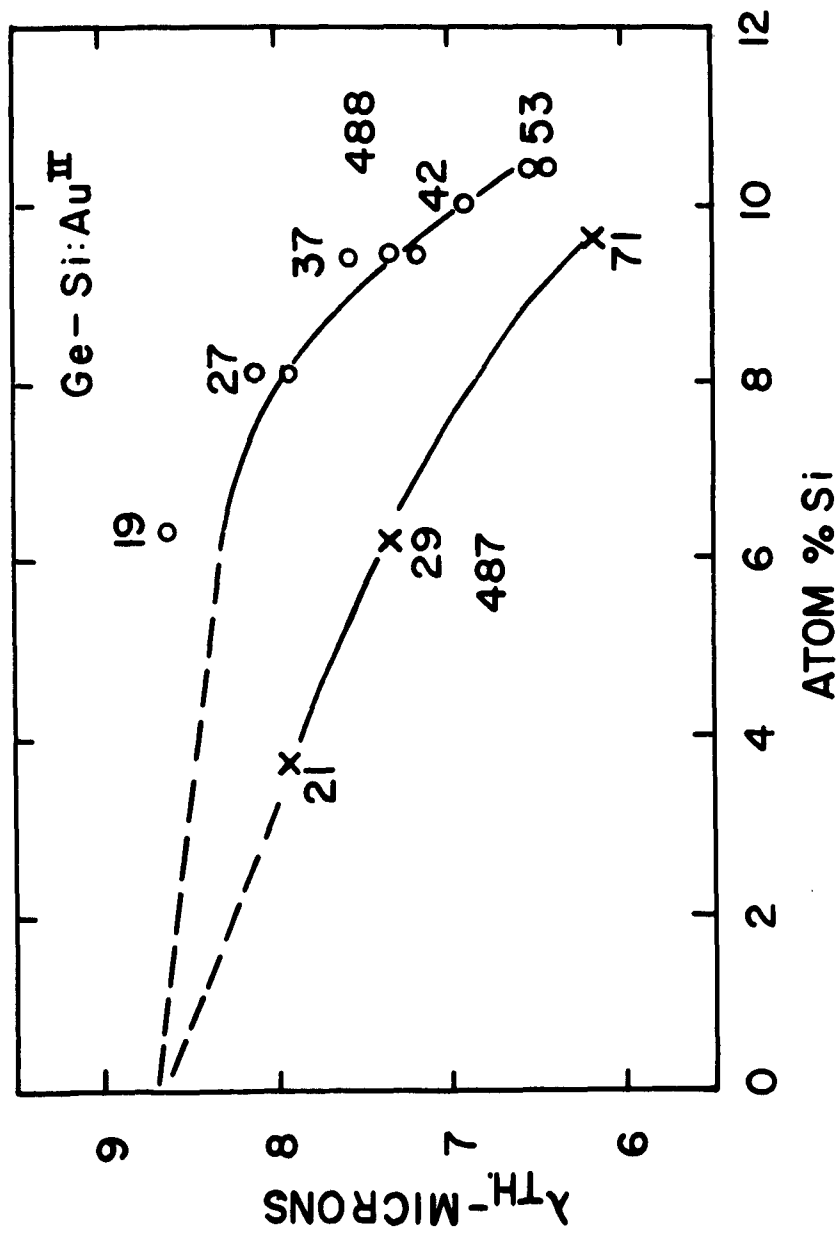


FIG.2

### B. Magnitude of Photocurrent

The effect of changes in the degree of compensation upon the magnitude of the photocurrent may be illustrated by data on a series of samples from crystal 488. The increase in conductivity due to radiation for the case in which the absorption of the radiation is small may be shown to be given by

$$\Delta\sigma = e\mu\tau\sigma_p(N_A - N_D)J \quad (2)$$

where  $e$  = electronic charge  
 $\mu$  = carrier mobility  
 $\tau$  = carrier lifetime  
 $\sigma_p$  = photon absorption cross section  
 $(N_A - N_D)$  = concentration of uncompensated gold centers  
 $J$  = incident photon flux density

The mobility, at 78°K, is determined primarily by alloy scattering and by ionized impurity scattering. Over the limited range of silicon content involved here, from about 6 to about 10 atom percent silicon, the change in mobility due to the change in alloy scattering with composition is about 60%. The mobility due to ionized impurity scattering varies approximately inversely as the ionized impurity concentration which, in turn, is determined by the compensating donor concentration. In crystal 488, this varies by a factor of about three over the portion of the crystal under consideration. The carrier lifetime, according to Eq.(5) is determined primarily by the compensator concentration. Therefore, for a given incident radiation flux,  $\Delta\sigma$  is expected to vary approximately as  $\left(\frac{N_A - N_D}{N_D^2}\right)$ . Fig. 3 gives the dependence of  $\Delta\sigma$  per watt of radiation at the peak wavelength of the extrinsic response upon this quantity. The concentration data for the samples used in this comparison are given in Table I. Each point represents the average of measurements on at least two samples. The solid line corresponds to proportionality between  $\Delta\sigma$  and  $\left(\frac{N_A - N_D}{N_D^2}\right)$ . The expected dependence of  $\Delta\sigma$  upon

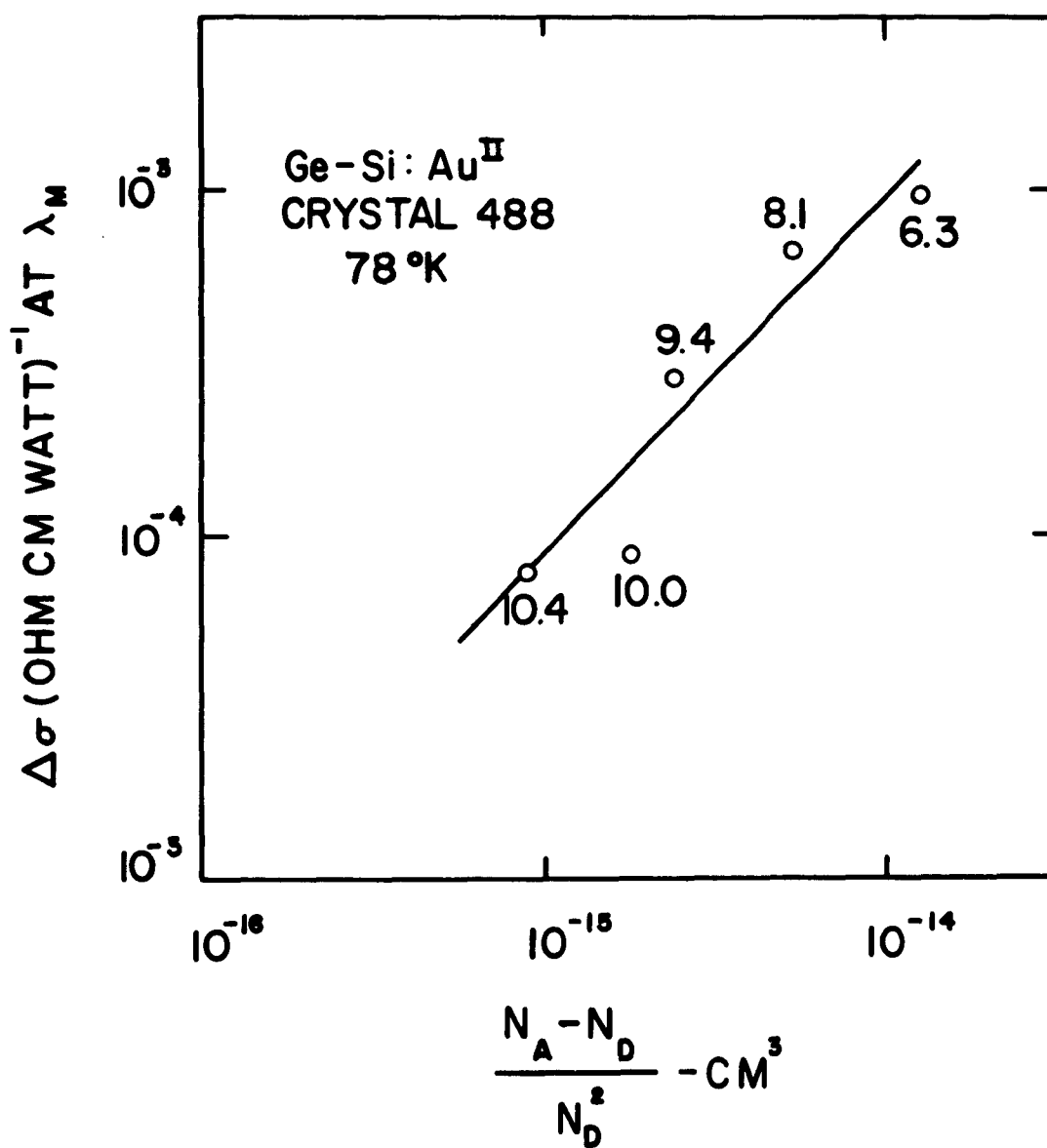


FIG. 3

activator and compensator concentrations appears to have been obtained with a precision which is probably determined by uncertainties in the knowledge of impurity concentrations. These results illustrate the importance of the need for accurate control of the degree of compensation of the activator impurity in order to maximize the responsivity.

TABLE I Ge-Si:Au <sup>II</sup> Samples Crystal 488			
Sample	Atom % Si	$N_A - N_D$	$N_D$
E	6.3	$1.51 \times 10^{15} \text{ cm}^{-3}$	$3.5 \times 10^{14} \text{ cm}^{-3}$
F	8.1	$1.36 \times 10^{15}$	$5.0 \times 10^{14}$
G	9.4	$1.17 \times 10^{15}$	$6.9 \times 10^{14}$
H	10.0	$1.08 \times 10^{15}$	$7.8 \times 10^{14}$
J	10.4	$0.87 \times 10^{15}$	$9.9 \times 10^{14}$

### C. Detectivities

Because of the excessive compensation of the samples of Ge-Si:Au<sup>II</sup> available, their detectivities were limited, for the most part, by non-fundamental noise sources. A typical curve of noise voltage versus bias voltage, given in the lower part of Fig. 4, illustrates the behavior observed. The noise remains at the zero bias value up to about 200 volts. Above this, the noise rises but very soon enters the range of excess noise. There is no well defined range in which the noise is proportional to voltage as should be the case for fundamental noise. If the material were properly compensated, the higher photoconductive gain which should be a consequence, would result in an increase both of the signal and of the noise. The noise from the sample, then, would rise above the zero bias noise at a lower bias voltage and generation-recombination or background

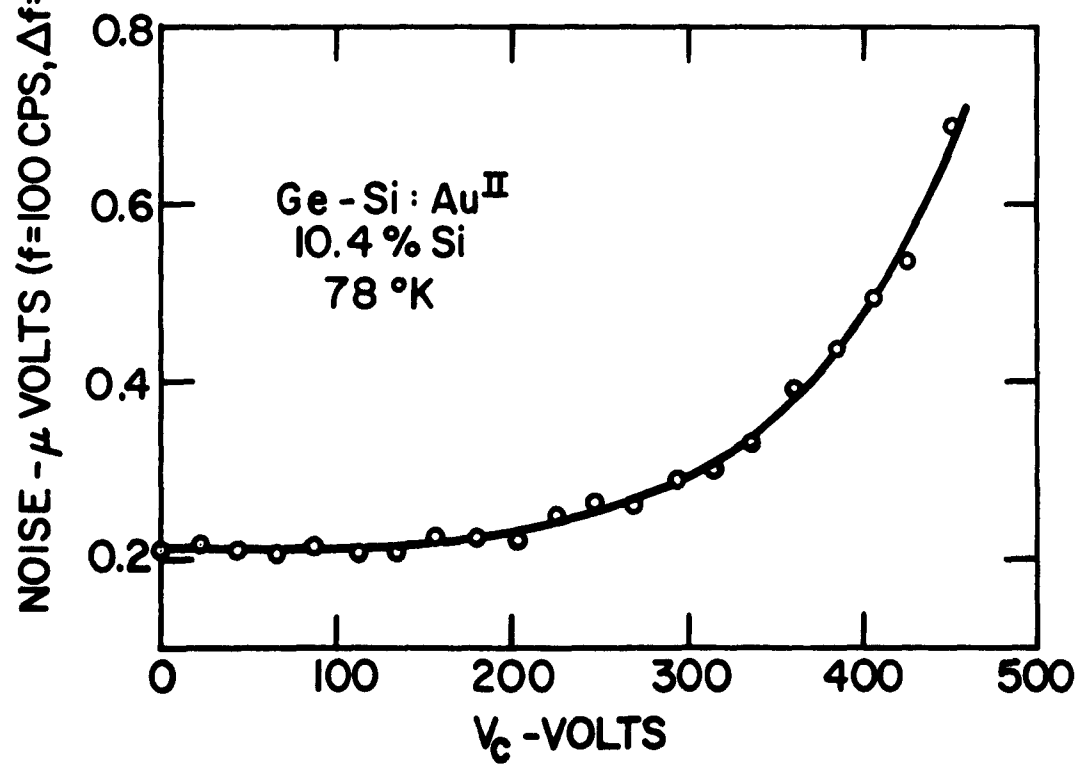
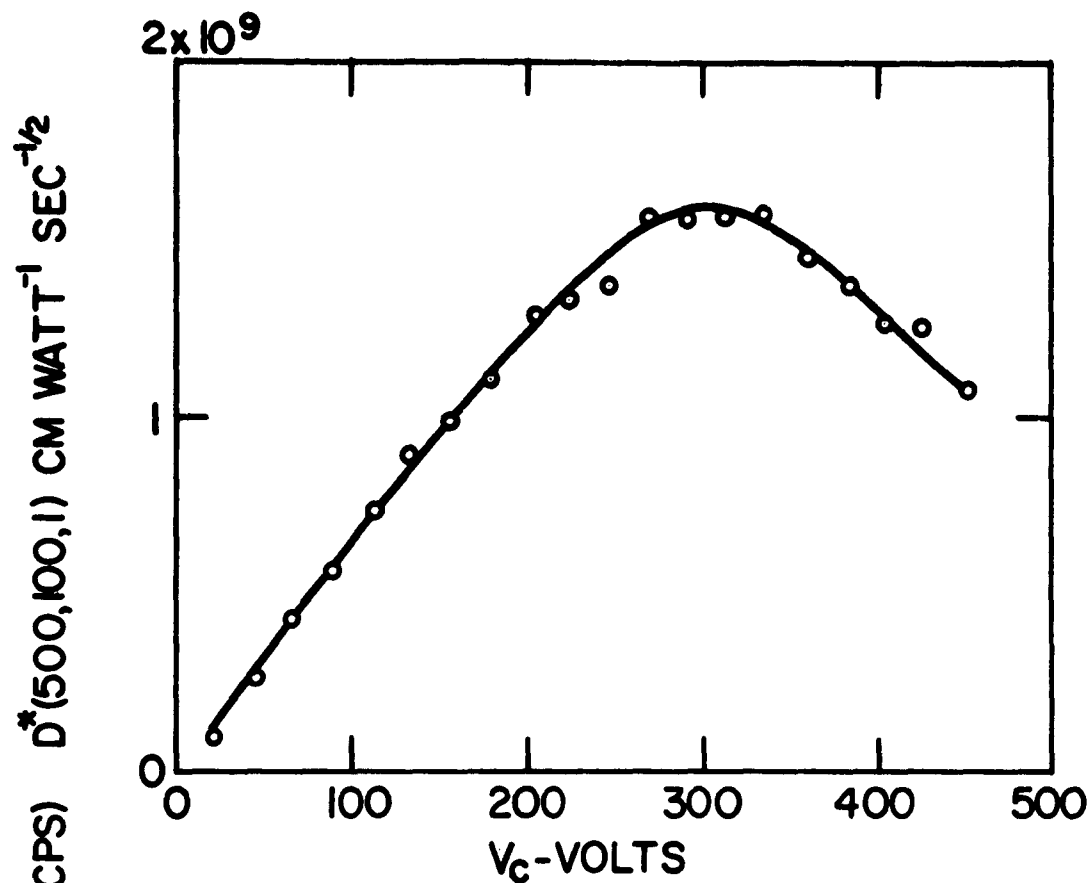


FIG.4

radiation noise limited operation, depending upon the operating conditions, would be obtained over an extended range of bias voltage. The 500<sup>o</sup>K black body D\* values are plotted as a function of bias voltage for the same sample in the upper curve of Fig. 4. The optimum bias is 310 volts and D\*(500,100,1) is  $1.6 \times 10^9$  cm watt<sup>-1</sup> sec<sup>-1/2</sup>,

The present state of development of the Ge-Si:Au<sup>II</sup> photoconductors is summarized in Table II in which D\* values for 500<sup>o</sup>K black body radiation, for the peak of the extrinsic response, and for 5 microns are given for the best sample at each of the alloy compositions investigated with crystal 488. For the first three samples, the expected increase of D\* values at constant operating temperature, 78<sup>o</sup>K, with shift of the threshold to shorter wavelengths is observed. The decrease of D\* value with increasing silicon content at the high end of the range is undoubtedly due to the noise situation described above. It is of interest

% Si	$\lambda_{Th}$ microns	D*(500,100,1) cm watt <sup>-1</sup> sec <sup>-1/2</sup>	D*( $\lambda_m$ ,100,1) cm watt <sup>-1</sup> sec <sup>-1/2</sup>	D*(5 $\mu$ ,100,1) cm watt <sup>-1</sup> sec <sup>-1/2</sup>
6.3	8.6	$2.1 \times 10^9$	$6.1 \times 10^9$	$6.1 \times 10^9$
8.1	8.0	$2.9 \times 10^9$	$1.0 \times 10^{10}$	$9.2 \times 10^9$
9.4	7.4	$3.7 \times 10^9$	$1.9 \times 10^{10}$	$1.4 \times 10^{10}$
10.0	6.9	$2.9 \times 10^9$	$1.6 \times 10^{10}$	$9.9 \times 10^9$
10.4	6.5	$1.6 \times 10^9$	$1.0 \times 10^{10}$	$5.6 \times 10^9$

to compare these results with expectation in terms of the relation between D\* and  $\lambda_{Th}$  given by Eq. (1). For the first three samples, which are not so badly overcompensated, the observed values are about a factor of three below the calculated. For the last two, for which the overcompensation is greatest, the factors are seven and thirty.

### III. Cobalt<sup>II</sup> Doped Germanium

The value for the ionization energy of the Co<sup>II</sup> level, the lowest lying acceptor state, is reported<sup>4</sup> to be 0.25 ± 0.01 ev. This was confirmed by measurement of the temperature dependence of resistivity of a cobalt doped sample, for which the curve of log resistivity versus inverse temperature is given in Fig. 5. The value of thermal ionization energy obtained was 0.25<sub>8</sub> ev. The corresponding photoconductive threshold should be 4.8 microns. The value observed for the wavelength at which the photoconductive response is a factor of ten below the extrinsic peak was 4.63 microns. The absolute spectral response of a sample at an operating temperature of 78°K is given in Fig. 6. The peak D\*(λ,100,1) value at 2.5 microns is 4.3x10<sup>10</sup> cm watt<sup>-1</sup> sec<sup>-1/2</sup>. The results of the measurement of the 500°K black body D\*(500,100,1) values at several different operating temperatures are given in Fig. 7. At high operating temperatures, log D\* increases with inverse temperature at a rate corresponding to 0.13 ev. This is just one-half of the ionization energy of the Co<sup>II</sup> level and is the value to be expected for generation-recombination noise limited operation. Below about 100°K, D\* is virtually temperature dependent. This is due, not to onset of background noise limited operation, but rather to a reduction of the noise below amplifier noise in the bias voltage range below noise breakdown. Here, as in the Ge-Si:Au<sup>II</sup> alloy, if the photoconductive gain can be increased by better adjustment of the compensation so that generation-recombination or background radiation noise limited operation can be obtained at lower temperatures, significant improvement in performance should be achievable.

The photocurrent, in amperes per watt of 500°K black body radiation incident on the sample, as a function of electric field across the sample for

---

4. W. W. Tyler, R. Newman, and H. H. Woodbury, Phys. Rev. 97, 669(1955).

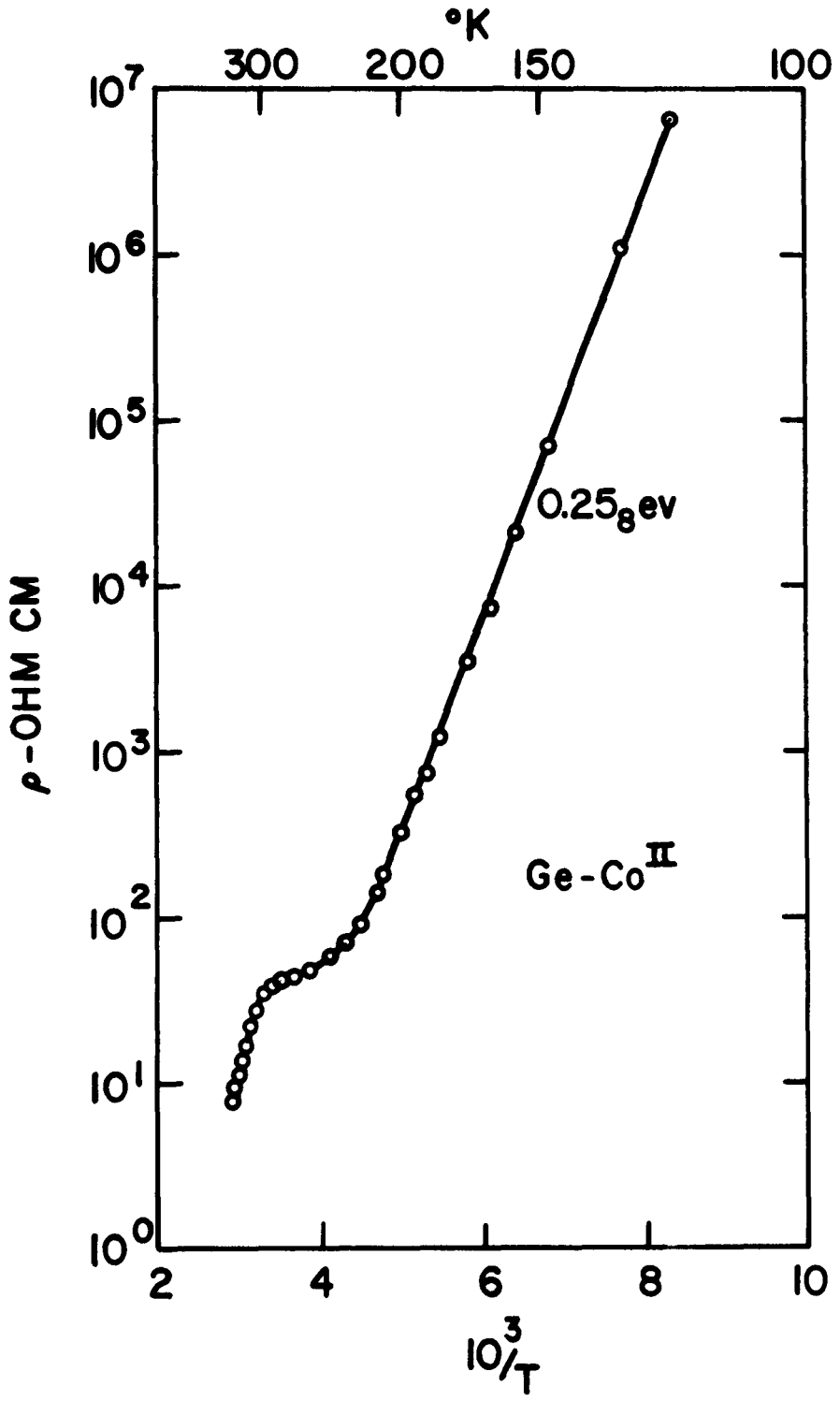


FIG. 5

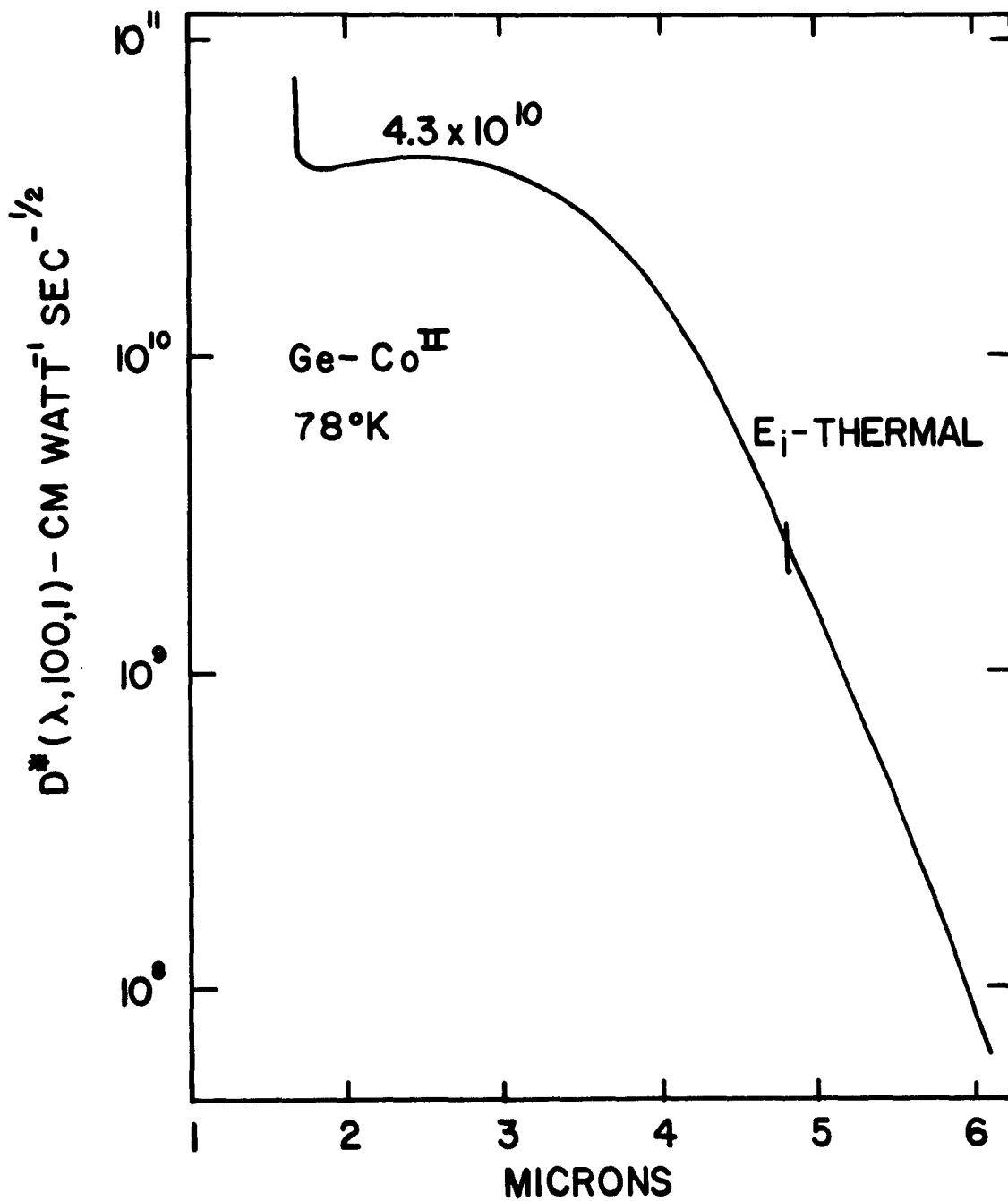


FIG. 6

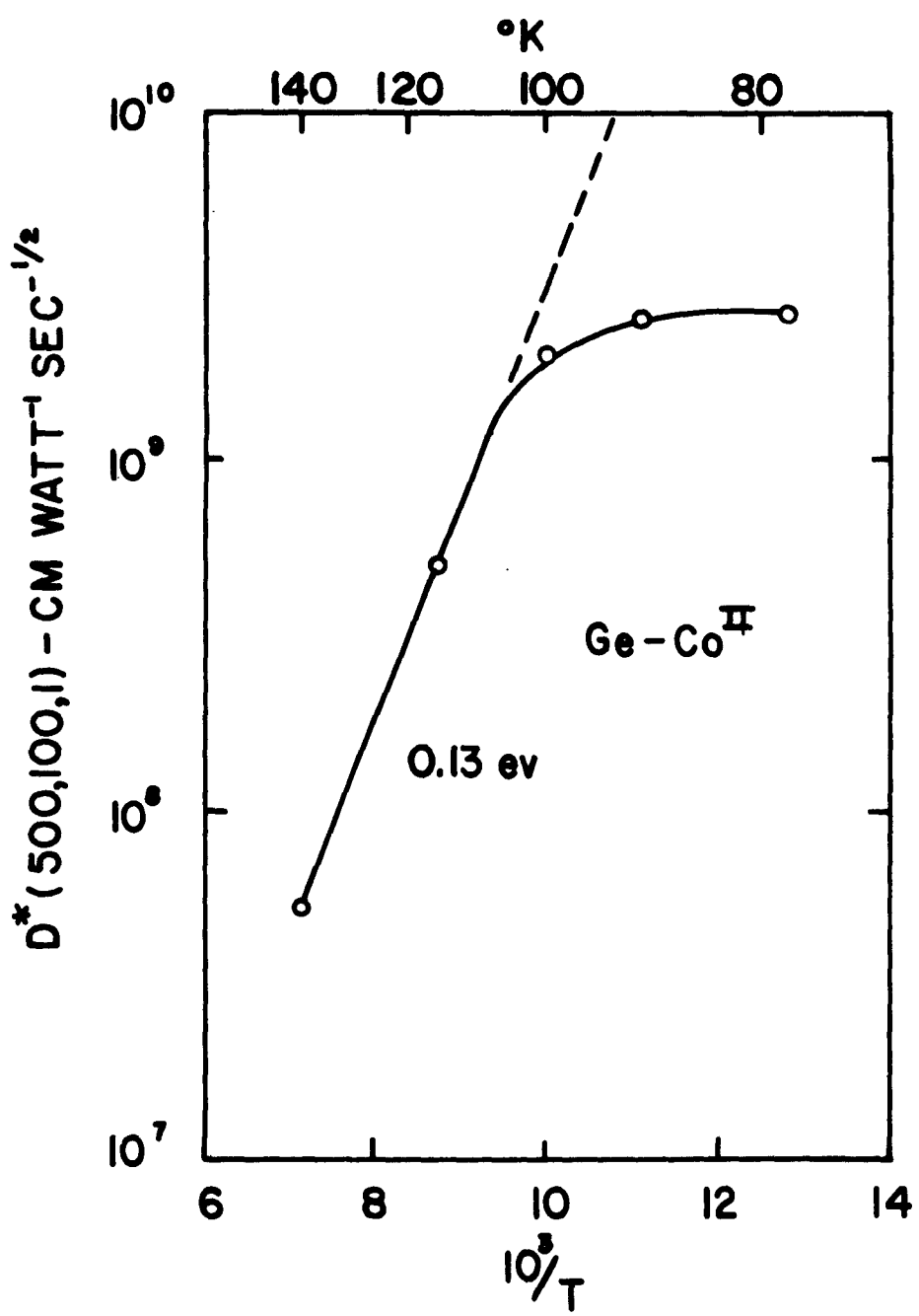
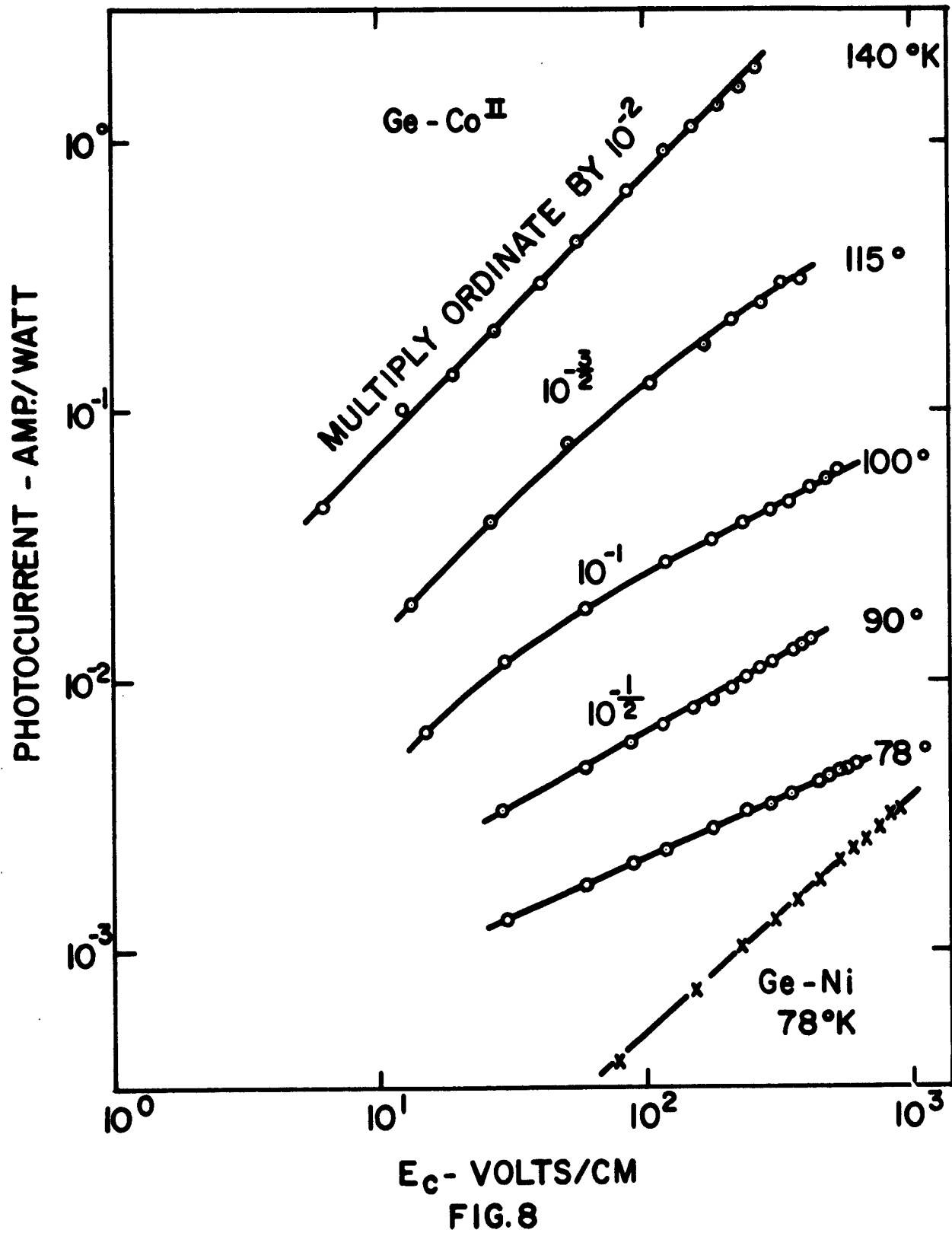


FIG.7

each of the sample temperatures investigated is given in Fig. 8. on a log-log plot. In order to separate the curves from one another, the ordinate scale has been shifted by half a decade from curve to curve. For the highest temperature,  $140^{\circ}\text{K}$ , the photocurrent varies linearly with field over the range investigated. At  $78^{\circ}\text{K}$  and  $90^{\circ}\text{K}$ , the current varies approximately as the square root of the field. At the intermediate temperatures, the dependence at low fields is linear while at high fields, the variation is less rapid and appears to approach a square root dependence. The field at which deviation from linearity sets in shifts to lower values as the temperature is decreased. Deviations from linearity, in the direction of sub-linearity, as great as this have not been observed with other extrinsic germanium or germanium-silicon alloy photoconductors. For comparison, a curve for nickel doped germanium at  $78^{\circ}\text{K}$ , plotted on the same scales as that for  $\text{Ge-Co}^{\text{II}}$  at  $78^{\circ}\text{K}$  is included. Here, the dependence of current on field is only slightly sub-linear, the exponent being 0.9. Unless this effect in  $\text{Ge-Co}^{\text{II}}$  is a spurious contact effect, which is believed not to be the case, it seems to indicate an electric field dependence of carrier mobility and/or lifetime which is specific for cobalt doped germanium.

The dependence of photocurrent upon radiation intensity for cobalt doped germanium at  $78^{\circ}\text{K}$  was investigated at several electric field strengths between 3 and 850 volts/cm. at two different wavelengths, 2.2 and 3.4 microns. In all cases, the photocurrent was proportional to the radiation intensity over a range of nearly four orders of magnitude variation of intensity. The data are reproduced in Fig. 9.



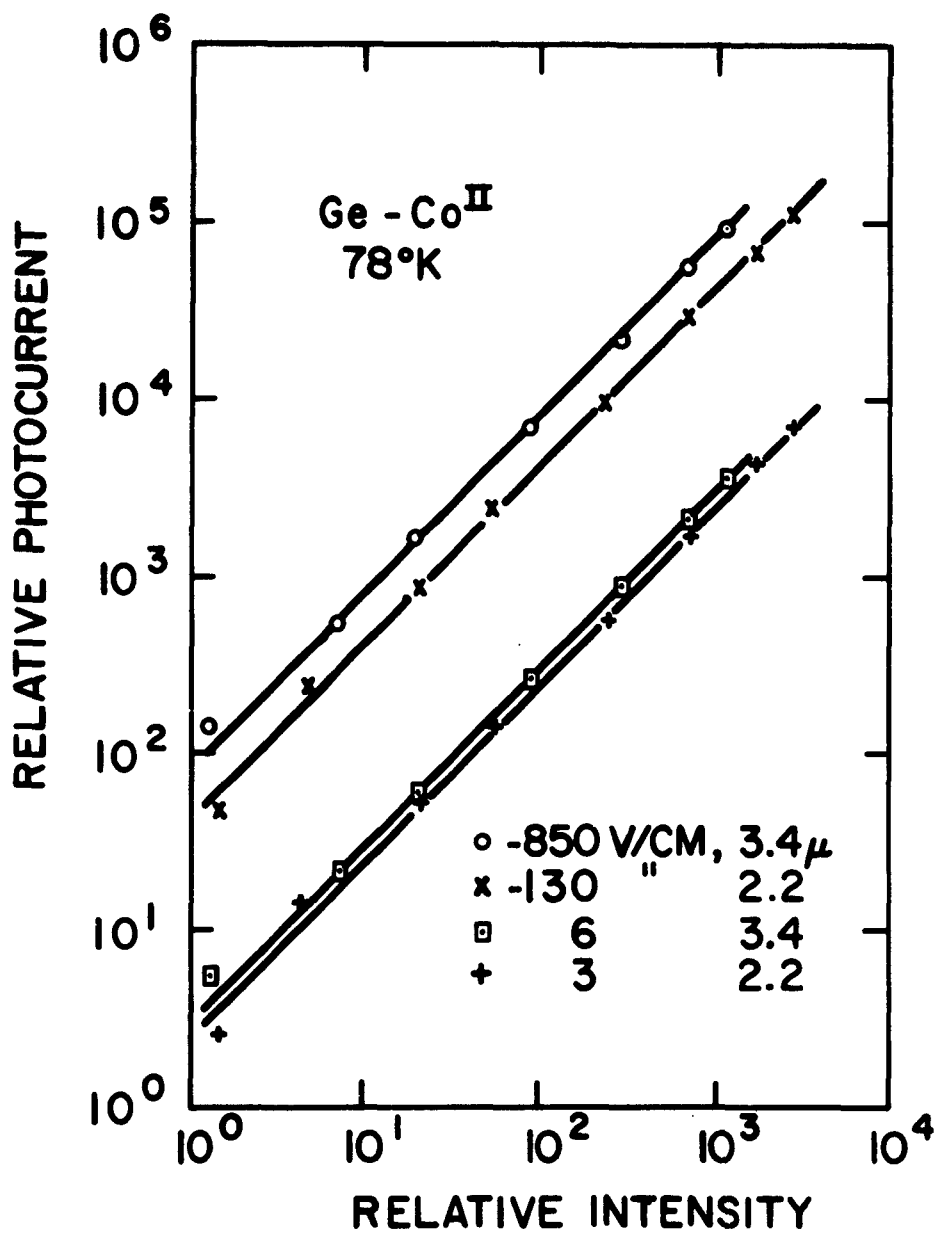


FIG. 9

#### IV. Nickel Doped Germanium

The lowest lying impurity level in nickel doped germanium is reported<sup>5</sup> to be an acceptor lying at  $0.22 \pm 0.01$  ev above the valence band edge. The thermal activation energy found in the present work, from measurement of the temperature dependence of resistivity of a nickel doped sample was  $0.23_6$  ev. This value corresponds to a photoconductive threshold at 5.3 microns. The value found experimentally was 5.25 microns.

The  $500^{\circ}\text{K}$  black body  $D^*(500,100,1)$  value of a nickel doped germanium sample at an operating temperature of  $78^{\circ}\text{K}$  was found to be  $1.8 \times 10^9$  cm watt<sup>-1</sup> sec<sup>-1/2</sup> at optimum bias. The dependence of noise and of  $D^*$  upon bias voltage for this sample is given in Fig. 10. The plot of photocurrent versus field for this same sample is given in Fig. 8. The absolute spectral response curve of the same sample appears in Fig. 11. As with the gold doped alloys and with cobalt doped germanium, the limitation on the  $D^*$  value is imposed by the low level of noise from the sample in the bias range below noise breakdown which, as has been pointed out before, is probably due to the unfavorable state of the degree of compensation of the activator impurity. It is not possible to estimate, as has been done for the gold doped alloys, the degree of compensation of either the Ni level or of the  $\text{Co}^{\text{II}}$  level or of the concentration of recombination centers in the samples measured since the concentration of shallow acceptor states due to annealing is not known. Because of this, it is difficult to estimate what improvement in performance of cobalt or of nickel doped germanium might reasonably be expected to be experimentally realizable. It is certain, however, that the performance attained in this preliminary study of these materials as reported here can be improved by significant factors by a more thorough investigation of the conditions of doping and compensation.

---

5. W. W. Tyler, R. Newman, and H. H. Woodbury, Phys. Rev. 98, 461(1955).

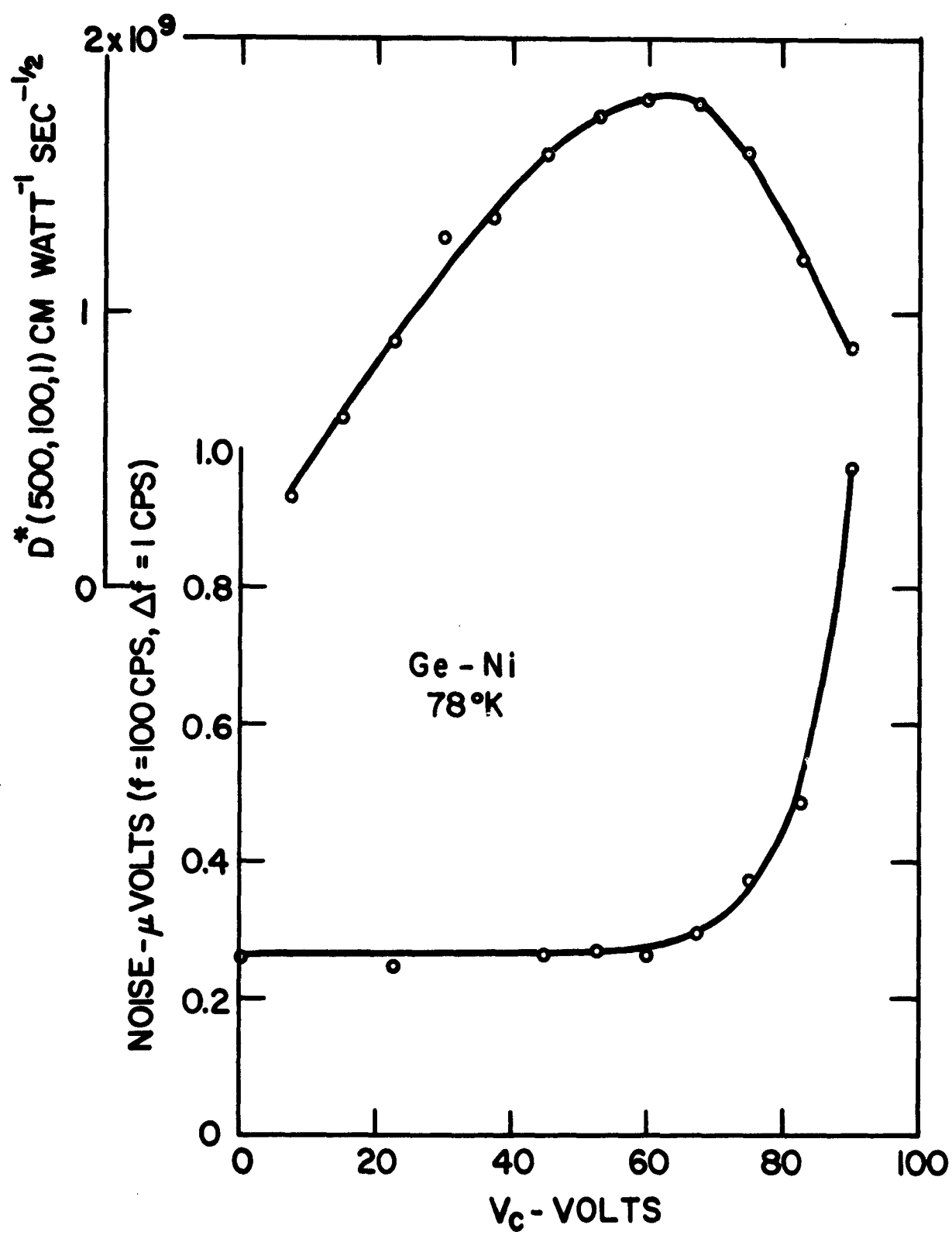


FIG. 10

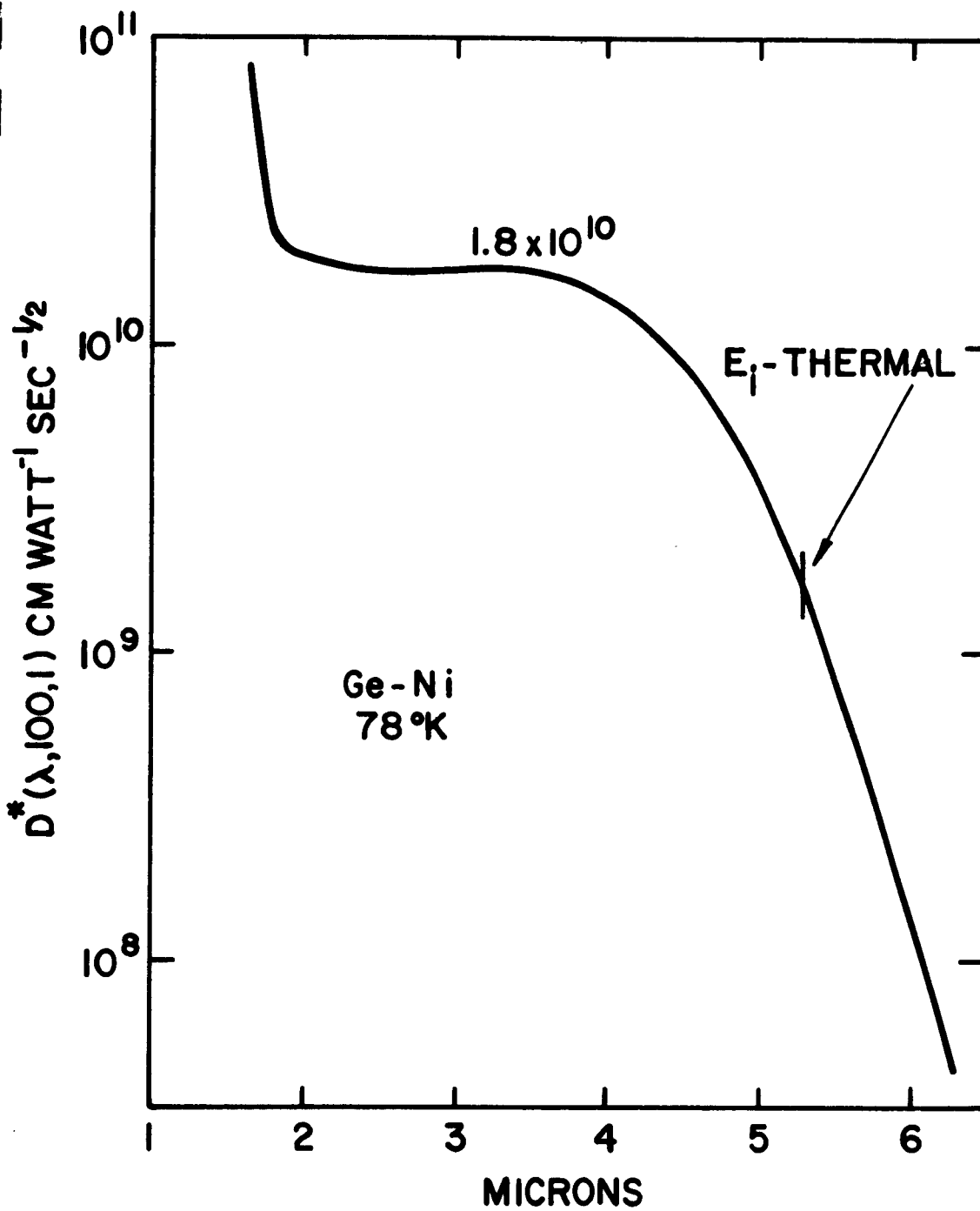


FIG. II

## V. Materials Preparation

### A. Gold Doped Germanium-Silicon Alloy

The general methods involved in the growth and doping of germanium-silicon alloy crystals have been described previously.<sup>1</sup> The crystals for the present work were grown by the horizontal zone melting technique in a manner such that there was a gradient both of silicon content and of concentration of compensating donor impurity in the growth direction of the crystal. The total gold concentration was maintained constant at about  $2 \times 10^{15} \text{ cm}^{-3}$ . Since, at the start of the investigation, neither the silicon content nor the concentration of compensating donor required were known accurately, the adoption of the crystal doping procedure used maximized the probability of obtaining some useful material from a given crystal with, however, the disadvantage that only a small portion of each crystal would be likely to be useful. The first crystals grown were greatly overcompensated. The results discussed above were obtained from two crystals, 487 and 488, both of which still were overcompensated in the silicon content range of primary interest. Time limitations prevented the improvement of compensation control beyond this point. Consequently, the results obtained do not represent the best possible performance of which the germanium-silicon-gold system is believed to be capable.

### B. Nickel Doped Germanium

The behavior of nickel in diffusion doping is similar to that of cobalt. Rapid annealing with the formation of low lying acceptors occurs to about the same extent in both. The achievement of optimum compensation of the 0.23 eV acceptor level is, therefore, subject to the same difficulty as in the case of cobalt. The experimental procedure in diffusion doping with nickel is like that described for cobalt.

C. Cobalt Doped Germanium

A description of the procedure used to prepare this material is discussed in Part II, Section II, paragraph B.

PART II  
COMPENSATED DONOR PHOTOCONDUCTORS

I. Introduction

The development of extrinsic germanium infrared photoconductors has reached the point where, by appropriate choice of activator impurity and conditions of compensation of the activator, virtually every portion of the spectrum between the visible and wavelengths of at least 100 microns may effectively be covered. In general, when cooled to operating temperatures low enough so that generation-recombination noise is negligible, these photoconductors exhibit radiation background noise limited operation and have values of detectivity within factors of the order of two to three of the theoretical. For those cases in which the measurements have been made, the primary quantum efficiency, in terms of absorbed photons, is close to unity. The principal area of improvement of these photoconductors is that of increasing their responsivity or photoconductive gain. An increase of responsivity increases the magnitude of the signal generated by a given radiation flux and the magnitude of the noise due to a given background radiation flux without altering the signal-to-noise ratio. The higher the signal and noise levels for a given signal-to-noise ratio, the less stringent are the conditions imposed upon the noise characteristics of the electronic circuitry associated with the photoconductive detector.

The semiconductor material parameters which determine the magnitude of the photoconductive gain are the carrier mobility and lifetime. The magnitudes of these quantities determine, for a given applied electric field, the average effective number of charge carriers which cross the interelectrode space in the photoconductor per carrier excited by absorption of a photon. At the temperature, at which most extrinsic germanium photoconductors must be operated, 77°K or below, the magnitude

of the mobility is determined primarily by impurity scattering. For the range of impurity concentrations usually encountered in extrinsic photoconductors, it is not likely that the mobility can be varied sufficiently by adjustment of activator impurity concentration or compensation, to produce large changes in the photoconductive gain.

The carrier lifetime, on the other hand, can be varied over several orders of magnitude. The lifetime is given by

$$\tau = \frac{1}{n v S} \quad (3)$$

where  $n$  is the concentration of states by which a free carrier may be captured;  $v$  is the thermal velocity of a free carrier and  $S$  is the capture cross-section of the state for a free carrier. In the case of what may be called a normal impurity center, a donor near the conduction band or an acceptor near the valence band,  $n$  is given by

$$n = n_m + n_{th} + n_{op} \quad (4)$$

where  $n_m$  is the concentration of minority compensating impurity;  $n_{th}$  is the concentration of thermally excited carriers and  $n_{op}$  is the concentration of carriers excited optically, either by background radiation or by the signal radiation. Equations (3) and (4) point out the need for minimizing the compensator concentration in order to maximize the lifetime. The compensator concentration cannot be reduced to zero, however, since then the Fermi level at low temperatures would be located near the midpoint in energy between the impurity level and the band edge rather than near the impurity level. In fact, it is virtually impossible to reduce the compensator concentration to a value below  $10^{12}$  to  $10^{13} \text{ cm}^{-3}$  since this is of the order of the minimum achievable concentration of residual impurities in germanium or silicon.

The term  $n_{th}$  in Equation (4) may be made small by cooling the photoconductor to a sufficiently low operating temperature. For any reasonable value of signal or of background radiation flux, the quantity  $n_{op}$  is several orders of magnitude smaller than that of  $n_m$ . Thus, Equation (3) may, to a high degree of approximation, be written

$$\tau = \frac{1}{n_m v S} \quad (5)$$

The lifetime for a normal impurity center, then, should be inversely proportional to the compensator concentration. In those cases for which this concentration can be made small; for example, copper doped germanium, high responsivity is achieved. A study<sup>6</sup> of the dependence of photoconductive gain in copper doped germanium upon minority impurity concentration has demonstrated approximate agreement with Equation (5).

The capture cross-section of an ionized impurity center for a charge carrier may be expected to depend upon factors which vary from impurity to impurity. In addition, the charge state of the ionized center should determine the nature of the interaction with the charge carrier and thus have an influence upon the capture cross section. For singly ionized normal impurity centers, the recombination processes are:



for donors, and



for acceptors. In both cases, there is a coulomb attraction between the ionized center and the charge carrier. This should lead to large capture cross sections for these processes.

A class of impurities for which such a coulomb attraction does not exist

includes those which have acceptor levels lying above the middle of the forbidden gap of the host semiconductor or donor levels lying below the middle of the gap. When such levels are properly compensated, the recombination involves capture of a charge carrier either by a neutral center or by a center of the same sign as that of the charge carrier. In the former case, there is no coulomb interaction and in the latter, there is a coulomb repulsion. Both situations should lead to capture cross sections much smaller than those of normal centers.

There are two examples known of impurities in germanium which have donor levels lying near the valence band. These include the  $\text{Co}^{\text{I}}$  level at  $0.08 \text{ eV}$ <sup>7</sup> and the  $\text{Au}^{\text{I}}$  level at  $0.05 \text{ eV}$ <sup>8</sup> above the valence band edge. Both of these are of interest as potentially useful infrared detector materials; cobalt for the 8 to 13 micron atmospheric window region and gold for the wavelength range out to about 25 microns. When these levels are compensated by addition of a suitable concentration of an acceptor impurity having a level lying closer to the valence band than the donor, they behave as pseudo acceptor levels. The photoionization process leading to photoconductivity involves the excitation of a bound hole from the compensated donor into the valence band. The process terminating the life of an excited carrier involves the recombination of a free hole with a center containing an electron and which is therefore neutral. The process may be represented by:



The capture cross-section of this type of center in gold doped germanium has been reported<sup>9</sup> to be  $3.8 \times 10^{-18} \text{ cm}^2$ . The corresponding value for the Au normal acceptor level at  $0.15 \text{ eV}$  above the valence band reported in the same paper was

7. W. W. Tyler, J. Phys. Chem. Solids 8, 59(1959)

8. W. C. Dunlap, Jr., Phys. Rev. 100, 1629(1955); H. H. Woodbury and W. W. Tyler, Phys. Rev., 105, 84(1957).

9. L. I. Neuringer and W. Bernard, Phys. Rev. Lett, 6, 455(1961)

$1.6 \times 10^{-12} \text{ cm}^2$ . These values were obtained by analysis of the frequency spectrum of generation-recombination noise of a gold doped germanium sample at a temperature,  $97^\circ\text{K}$ , at which the Fermi level was midway between the two gold levels. Values for the cross section of the 0.15 eV level reported by other investigators range between  $2.3 \times 10^{-14} \text{ cm}^2$  and  $4.9 \times 10^{-13} \text{ cm}^2$ . Although the spread in values is great, the available data indicate the existence of the effect of the charge of the recombination center upon the magnitude of the cross sections of the two types of centers. No data are currently available for cross sections of any cobalt levels.

The present investigations of cobalt and of gold doped germanium are concerned largely with the determination of the behavior of the compensated donor levels and with the interpretation of the observed effects in terms of a model for this type of photoconductor.

## II. Materials Preparation

### A. Gold Doped Germanium

In order to reveal the gold donor level lying near the valence band, it must be compensated by the addition, in a concentration nearly equal to that of the gold, of an acceptor impurity having a level lying closer to the valence band than does the gold level. In order to permit investigation of the effects of degree of compensation upon the photoconductive behavior, the melt doped crystals were grown in a manner such that, in a given crystal, the gold concentration was constant while the compensator (usually gallium) concentration increased approximately linearly along the crystal. This was accomplished by first growing, in a horizontal zone furnace, a germanium crystal having a constant gallium concentration along its length. An appropriate amount of gold and sometimes extra gallium was then added to the first zone length and the zone passed through the crystal a second time. Concentrations of gold and gallium in the finished crystal were estimated from four point probe resistivity measurements made at room and at liquid nitrogen temperatures.

### B. Cobalt Doped Germanium

The starting material used for diffusion doping of germanium with cobalt is determined by which level the 0.08 eV donor or the 0.25 eV acceptor is to be dominant. In the first case, it is necessary to have present, prior to diffusion, a concentration of shallow-acceptor sufficient to remove electrons from most, but not all of the cobalt donors. The principal problem associated with the preparation arises because of the rapid rate of removal of cobalt by annealing as the samples are cooled from the diffusion temperature, approximately 870°C. Low lying acceptor states are produced in a concentration which is roughly equal to the reduction in concentration of cobalt due to the annealing. Since these acceptor states remove electrons from the donor levels of the remaining substitutional

cobalt atoms, their presence must be taken into account in adjusting the concentration of deliberately added acceptor impurity prior to diffusion. For this reason, it is essential to minimize, by rapid quenching, the annealing of cobalt during cooling and to make the loss due to annealing as reproducible as possible from run to run.

The diffusion procedure involved first the preparation of a single crystal wafer of germanium about 2mm thick doped with the desired compensator impurity. This wafer was electroplated with a thin layer of cobalt and then heated in a furnace to the diffusion temperature. After heating for several hours in a purified dry helium atmosphere, the wafer was cooled by moving the boat out of the furnace hot zone and at the same time passing a rapid flow of helium gas cooled with liquid nitrogen through the furnace tube. Concentrations of the various types of centers present were determined from resistivity data on the material before cobalt doping and from analysis of temperature dependence of resistivity data taken over the range from 400°K to 65°K with bars cut from the wafers after cobalt doping. The maximum net concentration of the compensated donor level achieved was about  $1 \times 10^{15} \text{ cm}^{-3}$ .

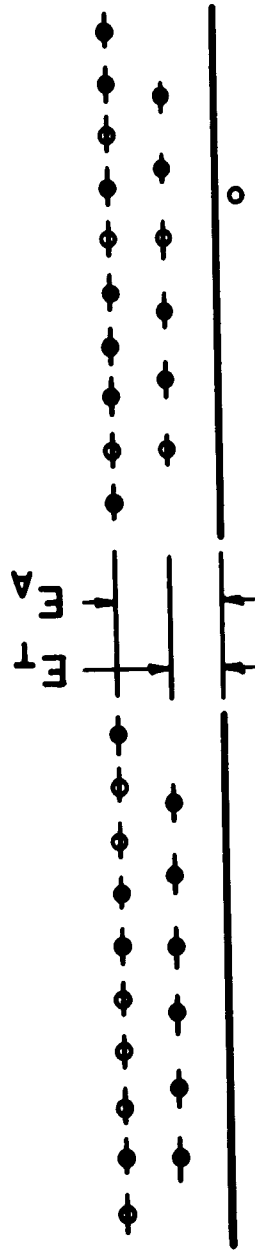
The procedure for preparation of cobalt doped germanium in which the 0.25 ev acceptor level is dominant is similar, except that the starting material now must be n-type rather than p-type in order that the low lying acceptors introduced by annealing are completely compensated. The uncertainty in the knowledge of the shallow acceptor concentration to be obtained in a given diffusion introduces a significant uncertainty in the adjustment of the initial donor concentration to give optimum compensation of the cobalt level. Even with rapid quenching, the concentration of low lying acceptors may be in excess of  $10^{14} \text{ cm}^{-3}$  which is roughly ten percent of the activator concentration.

### III. Model of Compensated Donor Photoconductor

The objective of the present section is the, principally qualitative, discussion of a model which appears to be capable of accounting for the main features of the behavior of compensated donor photoconductors of the type Ge-Co<sup>I</sup> or Ge-Au<sup>I</sup>. This behavior, to the extent that it has been thus far investigated, will be described in later sections.

The model to be considered includes an activator impurity level which is a donor lying at an energy  $E_A$  above the valence band edge and which is present in total concentration  $A$  and an acceptor impurity lying at an energy  $E_T$  ( $E_T < E_A$ ) above the valence band and which is present in total concentration  $T$  ( $T < A$ ). When such a material is in thermal equilibrium in the dark at a temperature low enough so that thermal ionization is negligible, the occupation of the levels is as schematically represented in Fig. 12-A. All of the acceptor levels are occupied by electrons from the activator donors leaving  $T$  holes and  $(A-T)$  electrons bound to the activator centers. Under these conditions, the material will exhibit photoconductive response only to radiation for which the photon energy is equal to or greater than  $E_A$ . However, once some holes have been photoexcited into the valence band, recombination can occur between these holes and either the acceptor states or the donor states containing electrons. The relative number of holes recombining in the two ways will be determined by the concentrations of the two types of recombination centers and their capture cross sections. If, as suggested in the Introduction, the donor states have small capture cross section, recombination into the low-lying states will be favored. Once an appreciable number of holes have been trapped on the low-lying states, photoionization of these can occur. If the radiation flux is maintained constant, a steady state distribution of bound holes between the two sets of levels will be established. Such a steady

CONDUCTION BAND



VALENCE BAND

A. - DISTRIBUTION IN DARK

B. - STEADY STATE DISTRIBUTION IN PRESENCE OF BACKGROUND RADIATION

FIG. 12

state distribution is represented schematically in Fig. 12-B. This would be the case, for example, if the material were exposed to a background radiation flux. Under these conditions, the material ought to exhibit photoconductive response with a threshold at a wavelength corresponding to  $E_T$  rather than to  $E_A$ . In other words, photoconductive response at wavelengths considerably longer than that corresponding to the normal threshold of the activator impurity should be observable provided that, in the steady state condition, the concentration of holes bound to the low-lying state is sufficiently large.

As the operating temperature of the material is raised above the low value assumed in the preceding discussion, thermal ionization of holes bound to the low-lying acceptor will become more and more probable until a temperature is reached for which the low-lying state is essentially completely ionized. Under these conditions, the low-lying state can no longer act as a recombination center. If, at the same time, the ionization energy,  $E_A$ , of the activator state is sufficiently larger than  $E_T$ , the activator will still not be appreciably thermally ionized. The material, then, will no longer exhibit photoconductivity at wavelengths greater than that corresponding to  $E_A$  but should exhibit photoconductivity at shorter wavelengths and should have a threshold at  $E_A$ .

There is one other very important implication of this model. If the compensated donor center does have a much smaller capture cross section than a normal acceptor center, the recombination, at low temperatures, will be dominated by capture into the low-lying acceptor. The lifetime, consequently, will be short and the photoconductive gain low. At temperatures high enough so that the low-lying acceptors are essentially completely thermally ionized but not so high that the deeper-lying compensated donor centers are appreciably thermally ionized, the recombination can no longer occur into the low-lying state but only into

the activator state. Since this is postulated to have a small capture cross section, the lifetime under these conditions should be long and the photoconductive gain high. If, then, the photocurrent excited by a given radiation flux is measured as a function of operating temperature, this photocurrent should show a large positive temperature coefficient in the range in which thermal ionization of the low-lying acceptor sets in and proceeds to completion. It is only in this relatively higher temperature range that the improvement in responsivity to be expected from the small capture cross section of a compensated donor center should be realizable.

As indicated in the qualitative discussion above, the existence of photoconductivity at wavelengths beyond the normal threshold of the activator impurity depends upon the establishment of a sufficient concentration of bound holes on the low-lying center in the steady state condition due to irradiation. An expression for this concentration will be derived for the case in which the temperature is low enough so that thermal ionization may be neglected. It will be assumed that the material is exposed to a constant background radiation flux corresponding to a black body at temperature  $t$ . The quantities involved in the analysis are defined as follows:

- $A$  = Total concentration of activator center
- $A_1$  = Concentration of activator centers containing bound holes
- $T$  = Total concentration of low-lying centers
- $T_1$  = Concentration of low-lying centers containing bound holes
- $p$  = Concentration of holes in valence band
- $P_A$  = Photon flux from background capable of ionizing holes from activator centers
- $P_T$  = Photon flux from background capable of ionizing holes from low-lying centers
- $\sigma_A$  = Photon absorption cross section of activator center
- $\sigma_T$  = Photon absorption cross section of low-lying acceptor center

$B_A$  = Recombination coefficient for capture of free hole by activator center

$B_T$  = Recombination coefficient for capture of free hole by acceptor center

$v$  = Volume of sample

$l$  = Length of sample in direction of propagation of the radiation

In the steady state, the rate at which holes are captured by a level is equal to the rate at which holes are ionized from that level by the radiation. This condition is expressed by the following equations:

$$B_A p(A - A_1)v = P_A \sigma_A A_1 l \quad (9)$$

and

$$B_T p(T - T_1)v = P_T \sigma_T T_1 l \quad (10)$$

If  $p$  is eliminated from Eqs. (9) and (10), an expression for the ratio  $T_1/T$  may be obtained.

$$\frac{T_1}{T} = \frac{P_A \sigma_A B_T A_1}{P_T \sigma_T B_A (A - A_1) + P_A \sigma_A B_T A_1} \quad (11)$$

If the following ratios are defined,

$$\frac{P_T}{P_A} = P, \quad \frac{\sigma_T}{\sigma_A} = \sigma, \quad \frac{B_T}{B_A} = B, \quad (12)$$

Eq. 11 reduces to

$$\frac{T_1}{T} = \frac{BA_1}{P\sigma(A - A_1) + BA_1} \quad (13)$$

There exists an additional relationship between  $T_1$  and  $A_1$ . The total concentration of holes in the system is  $(A_1 + T_1 + p)$ . This must be equal to  $T$ . For any reasonable background flux, the free hole concentration,  $p$ , is negligible compared with the other concentrations. Thus

$$A_1 = T - T_1. \quad (14)$$

When this is substituted into Eq. (13), the expression for  $T_1/T$  becomes

$$\frac{T_1}{T} = \frac{B(T-T_1)}{P\sigma(A-T+T_1) + B(T-T_1)} \quad (15)$$

If  $\frac{A}{T} = N$ , the solution of Eq. (15) may be written

$$\frac{T_1}{T} = \frac{P\sigma(1-N) - 2B}{2(P\sigma-B)} + \frac{\sqrt{[P\sigma(N-1) + 2B]^2}}{4(P\sigma-B)^2} + \frac{B}{P\sigma - B} \quad (16)$$

The relative occupation of the low-lying acceptor state by bound holes under background (or other) irradiation depends upon the ratios of activator and compensator concentrations, of recombination coefficients or capture cross sections, of photon absorption cross sections, and of photon fluxes.

In order to give some idea of the form of the functional dependence and magnitudes involved, Eq. (16) has been plotted in Fig. 13 for several values of the parameters. A value of  $P\sigma$  of two has been chosen since this corresponds approximately to the case of Ge-Co<sup>I</sup> for irradiation by room temperature background radiation. The activator level lies at about 0.08 ev and the acceptor level produced by annealing at 0.038 ev. If  $N$  is not much greater than unity, which corresponds to nearly complete compensation of the cobalt donor, the ratio  $T_1/T$  is greater than 0.1 even for small values of  $B$ . If, in fact, the capture cross section of the acceptor level is much larger than that of the compensated donor, corresponding to  $B \gg 1$ , then  $T_1/T$  is large even for relatively large values of  $N$ . The lowest curve, for  $P\sigma = 100$  and  $N = 2.0$ , is included to illustrate the effect of an increase in  $E_A$  and/or a decrease in  $E_T$  upon the distribution. Here, the value of  $B$  must be much larger than before in order to achieve comparable bound hole concentrations.

It is not possible, at present, to make reliable numerical estimates for actual samples since the  $B$ 's and  $\sigma$ 's are not known. It is evident, however,

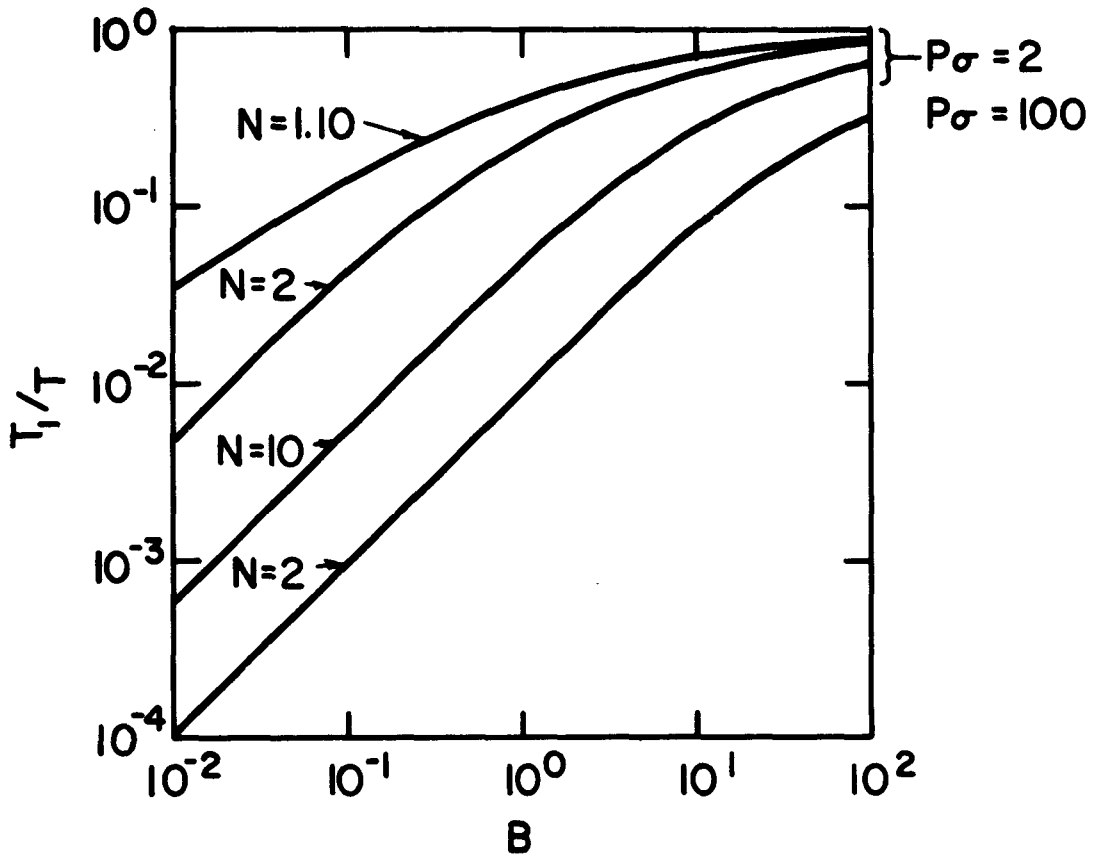


FIG. 13

that reasonable estimates of these parameters do give rise to a range of values of  $T_1/T$  which is adequate to account qualitatively for the excess photoconductivity which has been observed with Ge-Co<sup>I</sup> samples.

#### IV. Cobalt<sup>I</sup> Doped Germanium<sup>10</sup>

##### A. Energy Levels

The locations, in energy, of the impurity levels which are involved in the behavior of cobalt doped germanium as a compensated donor photoconductor were determined by measurement of the temperature dependence of resistivity of appropriately doped samples under conditions such that no external radiation was present. The curves of Fig. 14 are typical. Curve A was obtained from a sample for which the concentration of low lying acceptors was such that the cobalt donor level was partially but not completely compensated by loss of electrons to these acceptors. The slope corresponds to a thermal activation energy of 0.081 ev. This is slightly lower than the value, 0.09 ev, reported in the literature.<sup>7</sup> Samples examined during the course of this investigation have consistently given values in the neighborhood of 0.08 ev. When the combined concentration of deliberately added shallow acceptor and that due to annealing of cobalt is slightly greater than the cobalt concentration, behavior exemplified by curve B is observed. The slope, 0.038 ev, gives the thermal activation energy of the level introduced by the annealing of cobalt. If a sufficiently large excess of shallow acceptor, gallium or indium, had been added, a thermal slope of about 0.01 ev would have been observed. No such greatly overcompensated samples were investigated.

##### B. Black Body Photoconductive Response

The 500°K black body  $D^*$  values were determined under conditions such that the samples were exposed to room temperature background radiation entering the sample chamber through a 0.010 inch diameter aperture. The angular field of view for acceptance of background radiation was 19°. The  $D^*$  (500,100,1) values obtained at an operating temperature of 5.5°K are listed in Table III for two samples having different  $\text{Co}^{\text{I}}$  concentrations. Both  $D^*$  and  $\Delta\sigma_g$ , the change in conductivity per

---

10. A large fraction of the research reported in this section has been performed under Contract DA44-009-ENG-4863.

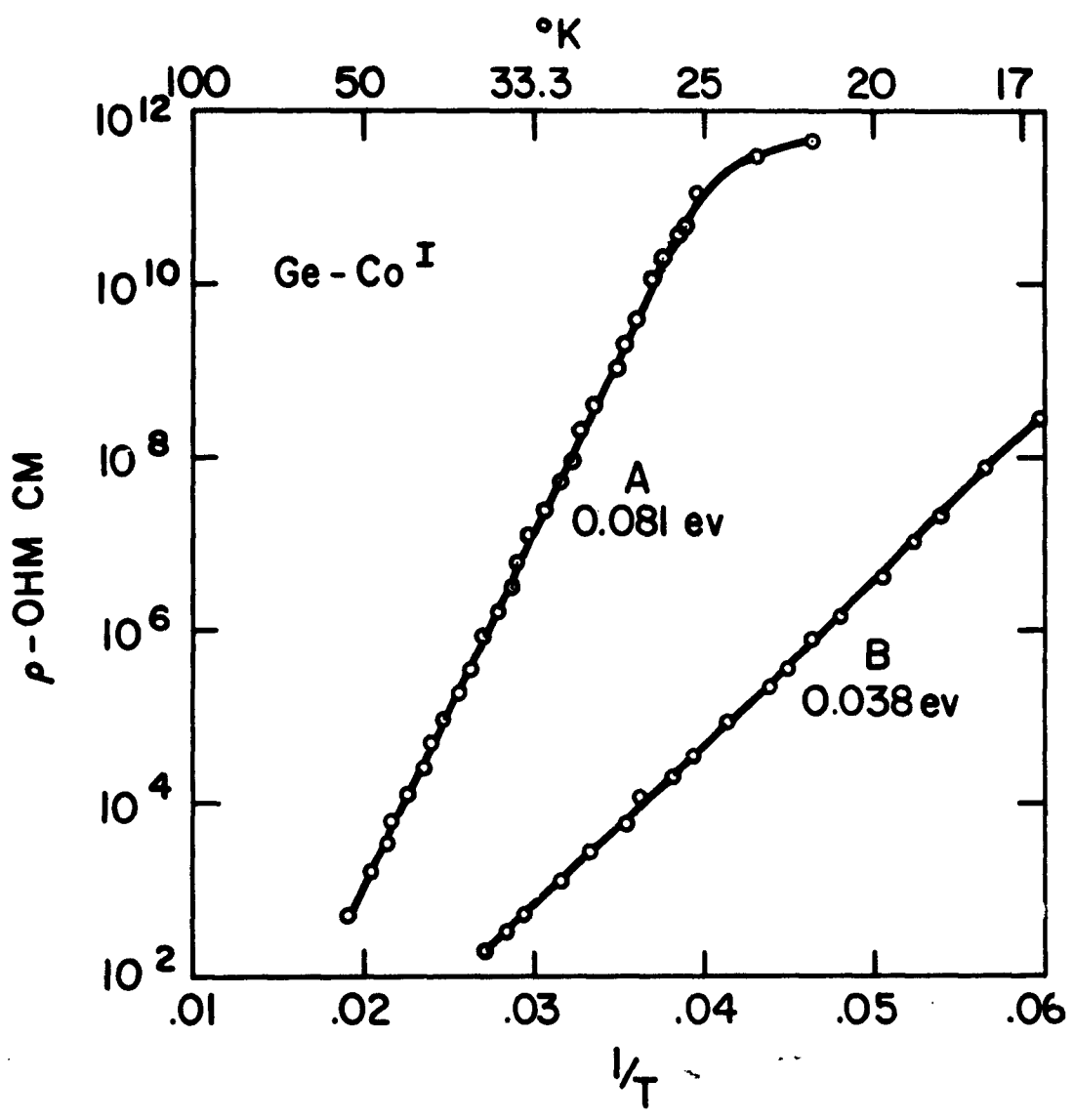


FIG. 14

Sample No.	505E	505H
Total Co conc., cm <sup>-3</sup>	1.5x10 <sup>15</sup>	1.3x10 <sup>15</sup>
Co <sup>I</sup> conc., cm <sup>-3</sup>	6.0x10 <sup>14</sup>	1.1x10 <sup>15</sup>
D*(500,100,1) cm watt <sup>-1</sup> sec <sup>-1/2</sup>	8.9x10 <sup>9</sup>	1.7x10 <sup>10</sup>
Optimum bias, volts	110	62
Δσ <sub>g</sub> , (ohm cm watt) <sup>-1</sup>	1.4x10 <sup>-3</sup>	3.0x10 <sup>-3</sup>

watt of 500°K black body radiation incident, are roughly proportional to the Co<sup>I</sup> concentration.

### C. Spectral Response Characteristics

The long wavelength threshold of photoconductivity of Ge-Co<sup>I</sup> is expected to lie at approximately 15 microns, corresponding to an ionization energy of about 0.08 ev. According to expectation based on the model of a compensated donor photoconductor discussed in the preceding section, this threshold should be obtained only at relatively high operating temperatures. The relative spectral response of sample 505H at 50°K is shown in Fig. 15. The extrinsic response is a factor of ten below its peak value at a wavelength of 14.5 microns. The shape of the curve at short wavelengths indicates the presence of a contribution from the second cobalt level at 0.25 ev above the valence band.

If the sample, however, is examined at operating temperatures low enough so that, because of the effect of background radiation, holes are trapped on the acceptor states lying below the cobalt donor level, the photoconductive response should extend to wavelengths longer than 15 microns. The response curve of the same sample, 505H, at 5.5°K is given in Fig. 16. At this temperature, photoconductivity extends to a wavelength of at least 25 microns which is the present long wavelength limit of the monochromator available. The approximate

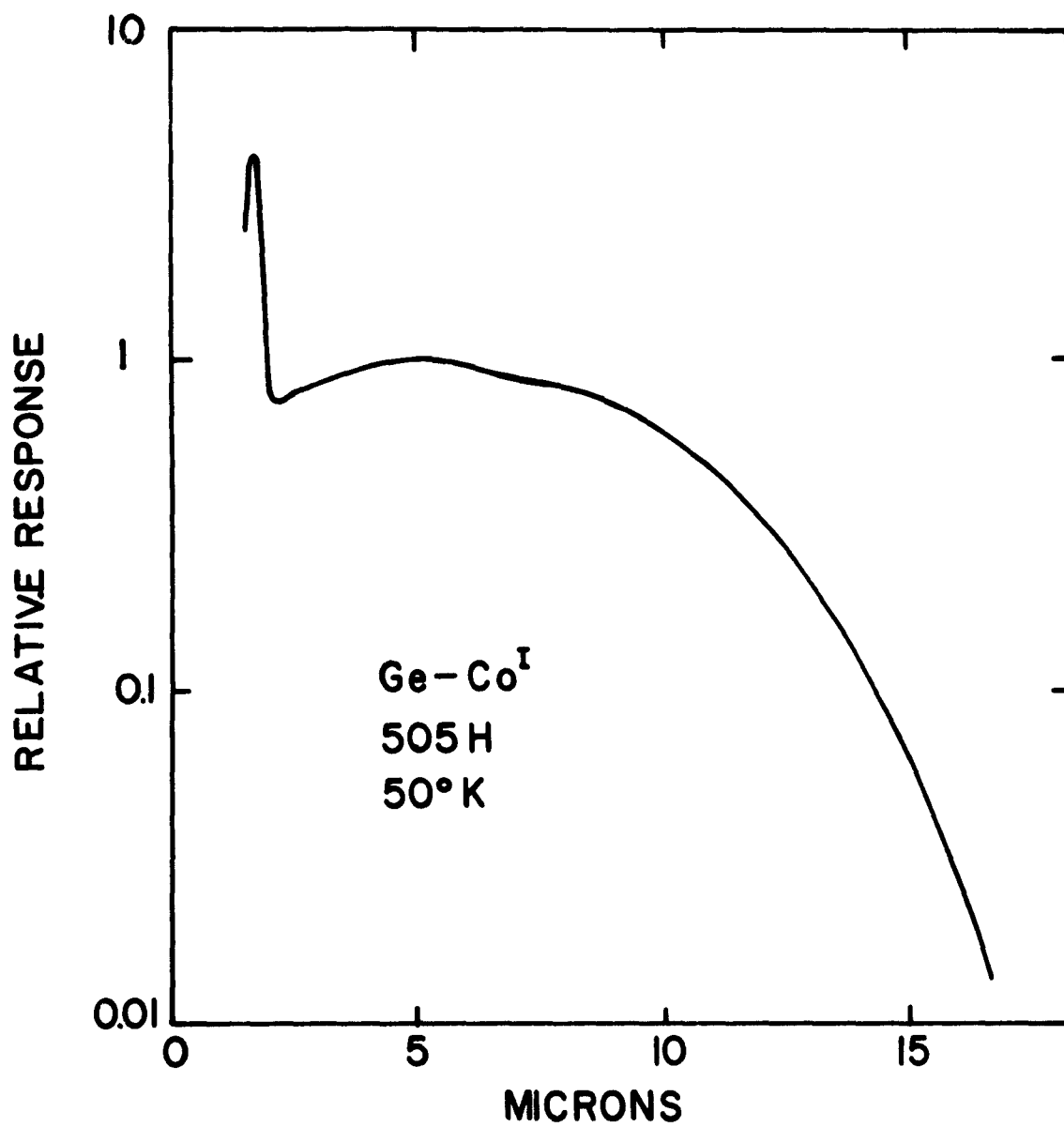


FIG. 15

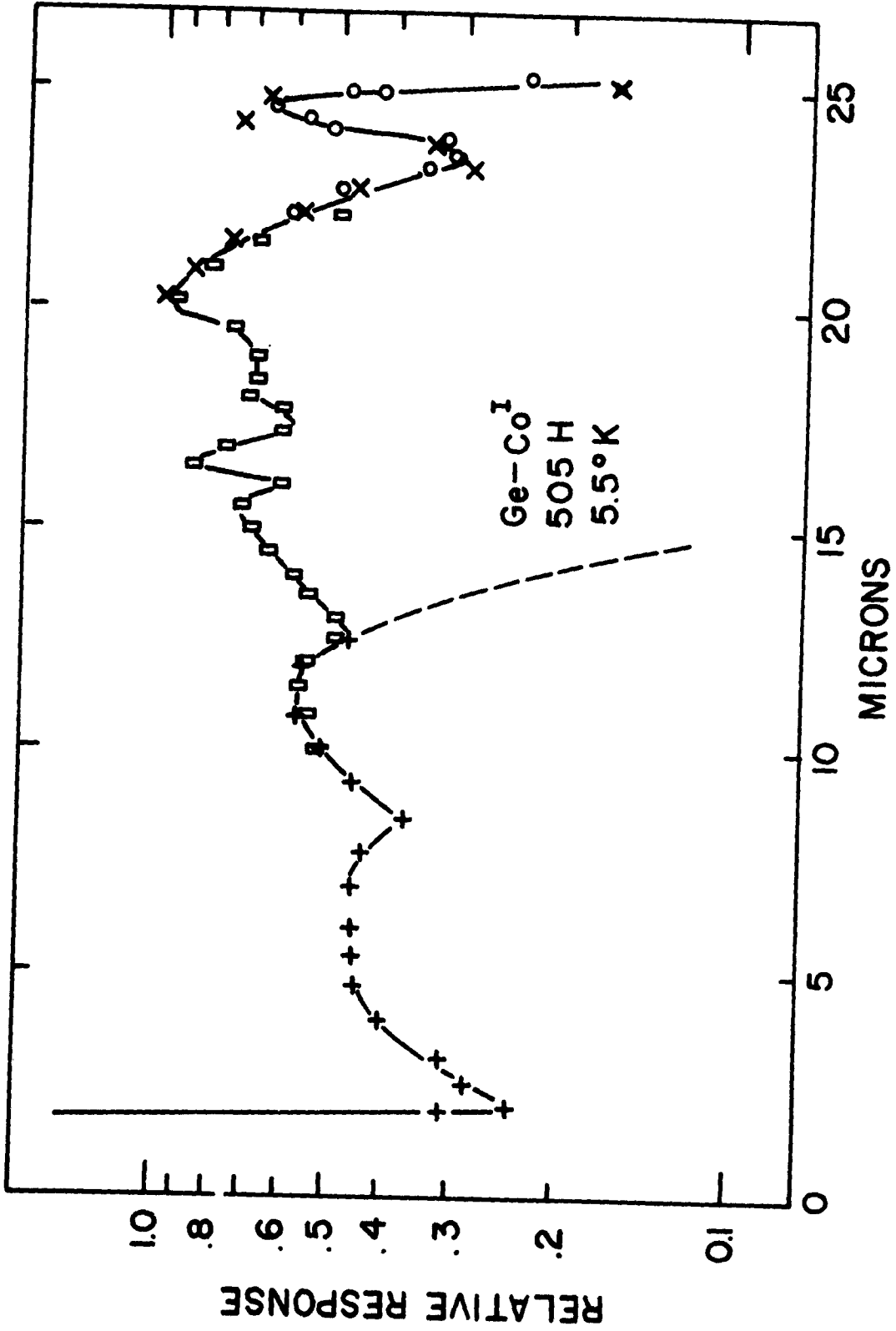


FIG.16

position of the normal  $\text{Co}^{\text{I}}$  threshold is indicated by the dashed line. The structure beyond 16 microns is due to lattice vibration absorption in germanium. Other samples have given spectra which are essentially identical except for some differences in detail. The spectral response behavior which has been observed is in qualitative agreement with prediction based on the model discussed above.

#### D. Temperature Dependence of Photocurrent

Two effects are expected to be observed in the investigation of the temperature dependence of the photocurrent in cobalt doped germanium. (1) The response, at wavelengths beyond the normal threshold, is expected to decrease, as the operating temperature is increased in going from a temperature at which the low lying acceptors containing holes are largely deionized to one at which these states are nearly completely ionized. (2) The photocurrent at wavelengths shorter than the normal threshold is expected to increase in the same temperature range in which the excess long wavelength response decreases provided that the product of capture cross-section and concentration of the recombination centers for the  $\text{Co}^{\text{I}}$  level is smaller than the corresponding produce for the shallow acceptor states.

The photocurrents at selected wavelengths, 5.3, 11.4, 15.0 and 20.2 microns, were measured as functions of temperature between  $5.5^{\circ}\text{K}$  and  $50^{\circ}\text{K}$ . The results obtained for sample 505H are shown in Fig. 17 in which the curves of relative photocurrent have been normalized to unity at  $5.5^{\circ}\text{K}$ . At 20.2 microns, the photocurrent is nearly temperature independent below  $20^{\circ}\text{K}$ . Above this temperature, it decreases rapidly by a factor of at least 100 until, at  $34^{\circ}\text{K}$ , no response is detectable above the noise. At 15.0 microns, the low temperature behavior is like that at 20.2 microns. Above  $32^{\circ}\text{K}$ , however, the response rises somewhat and ultimately levels off near  $50^{\circ}\text{K}$ . The behavior at 20.2 microns and the low temperature behavior at 15.0 microns represents that characteristic of effect (1) above. Appreciable fractions of the holes bound to the shallow levels become thermally ionized at temperatures

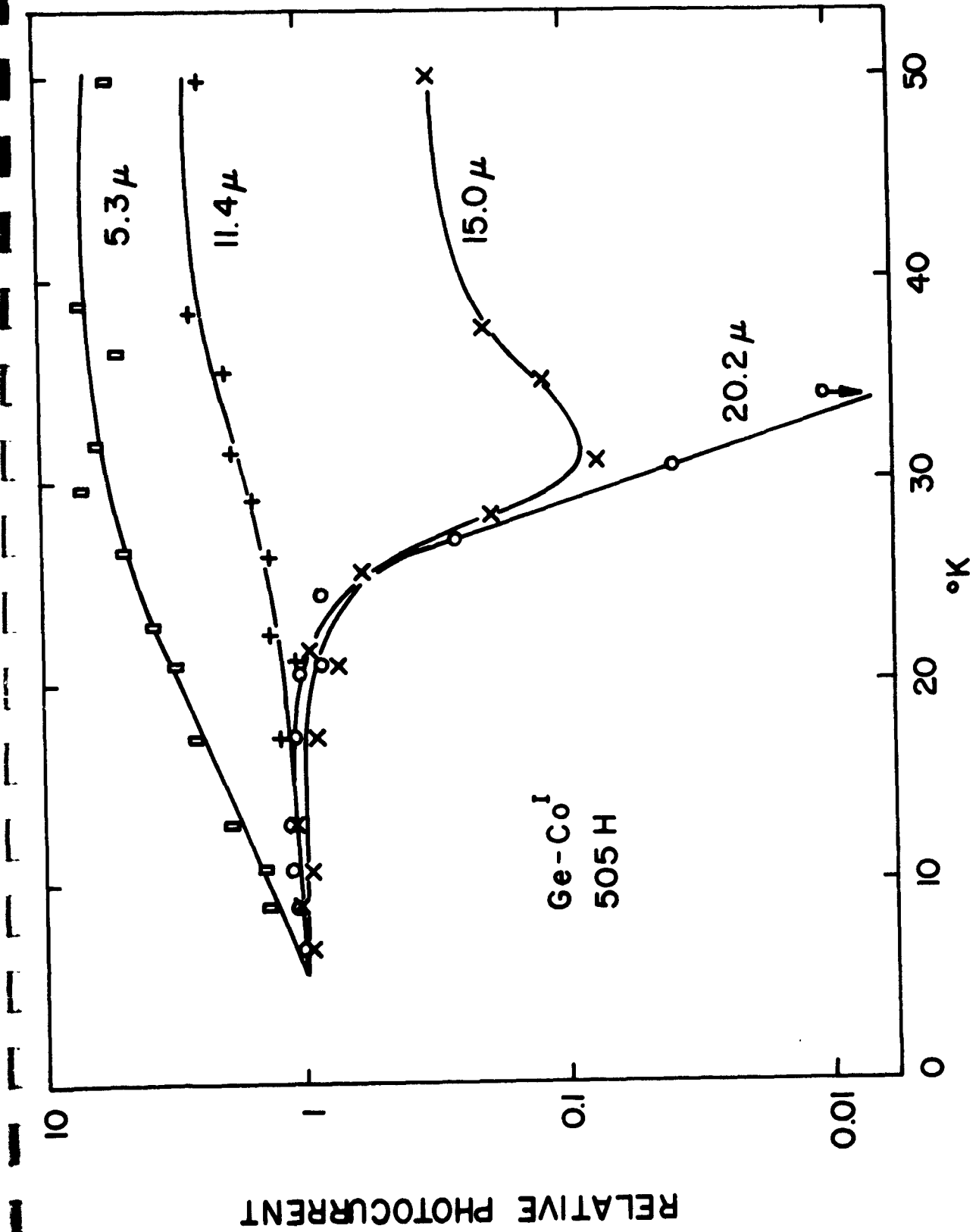


FIG.17

extending upward from about 20°K. This temperature range for extensive thermal ionization is about that to be expected considering the value reported above, 0.038 ev, for the thermal activation energy of the acceptor level. The rise in photocurrent with temperature in the high temperature range at 15.0 microns is probably due to the shift to longer wavelengths with rising temperature of the normal photoconductive edge.

The temperature coefficients of photocurrent at 5.3 and 11.4 microns, both of which lie within the normal extrinsic response range for  $\text{Co}^{\text{I}}$ , are positive over the entire temperature range. This is the type of effect to be expected for (2) above if the capture cross-section of the donor level for holes is smaller than that of the acceptor level. The magnitude of the increase, a factor of six at 5.3 microns and a factor of three at 11.4 microns, however, is considerably smaller than might reasonably be expected for a large ratio of the two cross-sections. Data on other samples with different degrees of compensation of the cobalt level are required in order to obtain a more comprehensive idea of the reliability of the low cross-section hypothesis.

#### E. Relative Quantum Yields

The relative magnitudes of the photocurrents in the wavelength range below 15 microns as compared with those at longer wavelengths are determined, according to the model, by the distribution of bound holes between the  $\text{Co}^{\text{I}}$  level and the lower lying acceptor level. It is not possible at present to calculate this distribution from Eq. (16) since the values of some of the required parameters are not known. The experimental results, however, can be used to obtain some idea of the distribution.

The relative photocurrents per incident photon at each of the selected wavelengths have been computed for the two samples of Table III. The results are

presented in Table IV. For each sample separately, the photocurrents per photon at an operating temperature of  $5.5^{\circ}\text{K}$  are the same to within a factor of approximately two at all of the selected wavelengths. Unless the photon absorption cross-sections are widely different at long and at short wavelengths, which is unlikely, the approximate constancy of the photocurrent per photon indicates that the concentration of holes bound to the low-lying states responsible for the long wavelength photoconductivity is about equal to that giving rise to the photocurrent at shorter wavelengths.

TABLE IV			
Ge:Co <sup>I</sup> - Photocurrents per Incident Photon			
T = 5.5°K			
Wavelength Microns	Photocurrent Arbitrary Units		Photocurrent Ratio
	505E	505H	505H/505E
20.2	1.43	2.88	2.01
15.0	1.56	2.95	1.89
11.4	1.72	3.21	1.87
5.3	2.22	6.76	3.04
Co <sup>I</sup> concentration ratio, 505H/505E=1.83			

When the two samples are compared, it is seen that the ratio of photocurrents at a given wavelength is very closely equal to the ratio of Co<sup>I</sup> concentrations in the two samples. The only large discrepancy occurs at 5.3 microns. Since, at this wavelength, the Co<sup>II</sup> level at 0.25 eV probably makes a significant contribution to the total photocurrent, this discrepancy should be assigned relatively little weight. The results of these two comparisons indicate the approximate equality of the concentrations of holes bound to the two types of centers. This conclusion is in qualitative agreement with the prediction of the ratio of these concentrations on the basis of Eq. 16 with the assumption that B is of the order of unity or larger.

## V. Gold<sup>I</sup> Doped Germanium<sup>11</sup>

### A. Temperature Dependence of Resistivity

The gold-gallium doped germanium available for this investigation includes crystals for which the total gold concentration has several fixed values between about  $2 \times 10^{14} \text{ cm}^{-3}$  and about  $1 \times 10^{16} \text{ cm}^{-3}$ . At each gold concentration, the range of gallium concentration is such that the net Au<sup>I</sup> concentration varies between a value close to that of the total gold and values of about one-half to one-tenth of the total gold.

Measurement of the temperature dependence of resistivity of samples from these crystals under conditions of no external radiation has indicated the existence of some apparently anomalous effects at the higher gold concentrations. Curve A of Fig. 18 is typical of the behavior of a normal sample. The resistivity increases exponentially with inverse temperature at a rate corresponding to the thermal ionization energy of the Au<sup>I</sup> level. When the resistivity becomes very high, about  $10^{11} \text{ ohm cm}$ , an apparent deviation from this exponential dependence occurs such that the apparent resistivity becomes nearly temperature independent. This behavior may be due to a slight residual trace of stray background radiation but may just as well be due to electrical leakage in the measuring system. Curve B of the same figure illustrates the behavior of a sample which is overcompensated with gallium. The slope, 0.014 ev, is approximately that to be expected for the gallium acceptor level. The gold concentration in the crystal from which these samples were obtained is about  $6 \times 10^{14} \text{ cm}^{-3}$ .

The curves of Fig. 19 illustrate the behavior of two samples from a crystal in which the gold concentration is considerably higher,  $3.1 \times 10^{15} \text{ cm}^{-3}$ . The behavior is normal up to resistivities of  $10^7$  to  $10^8 \text{ ohm cm}$ . Beyond this,

---

11. A portion of the research reported in this section has been performed under Contract AF33(657)-7864.

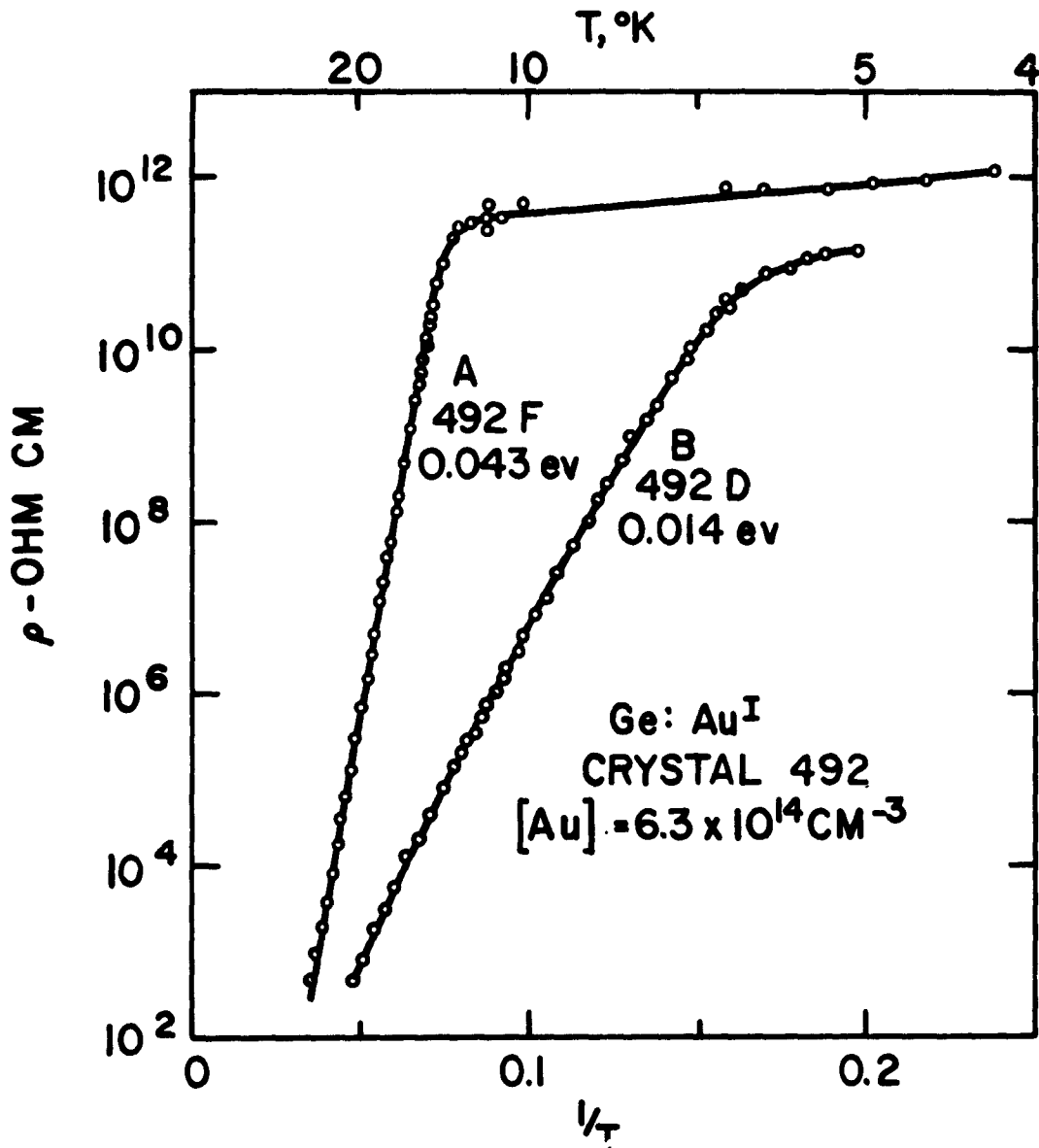


FIG. 18

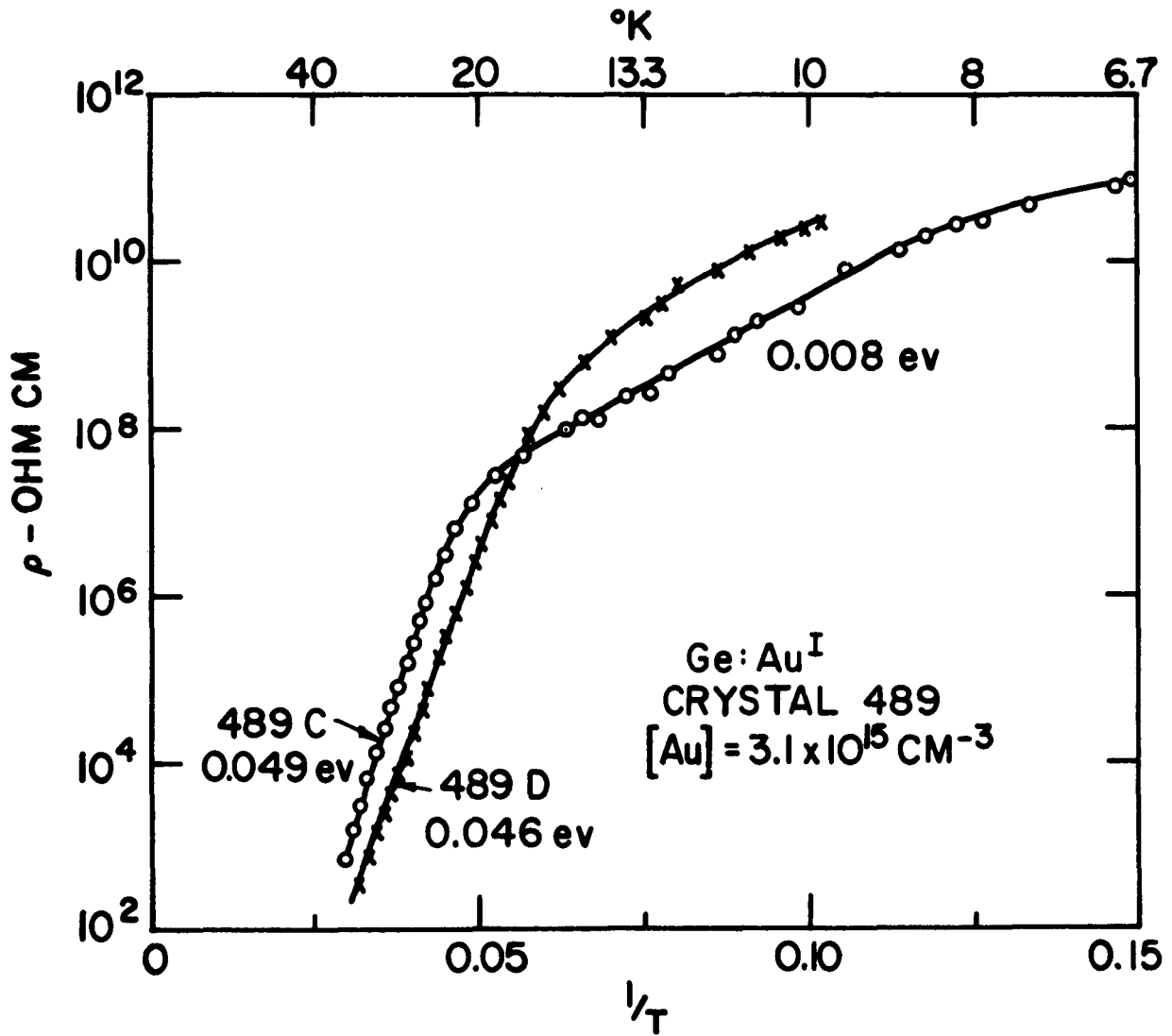


FIG. 19

the curves bend over and have slopes which are considerably smaller than would correspond to the presence of a slight gallium excess. For this reason, it is unlikely that the observed behavior is due to slight overcompensation of the gold level. This hypothesis would also be inconsistent with concentration data obtained from four point resistivity probe measurements made on the crystal before the samples were cut. It is, perhaps, more likely that the effect is due to impurity banding. This would be consistent with the absence of such effects at the lower gold concentrations. The investigation, thus far, has been confined to samples which do not exhibit this type of behavior.

#### B. Black Body Photoconductive Response

The 500°K black body  $D^*$  values, for two Ge:Au<sup>I</sup> samples, determined under the same conditions as those enumerated in Section IV-B, are given in Table V. The background noise limited  $D^*$  value is essentially the same for these two samples

Sample No.	492A	492F
Total Au conc., cm <sup>-3</sup>	6.4x10 <sup>14</sup>	6.3x10 <sup>14</sup>
Au <sup>I</sup> conc., cm <sup>-3</sup>	3.4x10 <sup>14</sup>	5.7x10 <sup>14</sup>
$D^*(500,100,1)$ cm watt <sup>-1</sup> sec <sup>-1/2</sup>	2.1x10 <sup>10</sup>	1.7x10 <sup>10</sup>
Optimum bias, volts	40	15
$\Delta\sigma_g$ , (ohm cm watt) <sup>-1</sup>	1.2x10 <sup>-2</sup>	3.5x10 <sup>-2</sup>

although there is a considerable difference in the compensation of the gold level in the two. The value of  $\Delta\sigma_g$ , however, does depend upon the Au<sup>I</sup> concentration. It may be noted that the  $\Delta\sigma_g$  values for these gold doped samples are about a factor of ten larger than those of the cobalt doped samples of Table III in spite of the fact that the net activator concentrations are somewhat smaller in the gold than in the cobalt doped samples.

### C. Spectral Response Characteristics

A typical spectral response curve for Ge-A<sub>1</sub><sup>I</sup> at an operating temperature of 5.5°K in the presence of background radiation is given in Fig. 20. The peak of the response occurs at about 17 microns and the apparent long wavelength threshold at about 25 microns, which is the value to be expected for an ionization energy of about 0.05 ev. The structure at wavelengths longer than 15 microns is due to germanium lattice vibration absorption. It has not yet been possible, for instrumental reasons, to search for the expected response beyond the normal threshold due to the background radiation induced redistribution of holes between the gold and the gallium levels. The threshold at about 25 microns may be only apparent and may be due to the presence of the very strong lattice vibration absorption peaking at about 29 microns. It will be necessary to investigate the wavelength range beyond about 35 microns in order to determine whether or not the response beyond the normal threshold is present. This will be done as soon as appropriate prisms for the Leiss monochromator are acquired.

### D. Temperature Dependence of Photocurrent

In the discussion presented in Section III, it has been pointed out that the existence of a small capture cross section for the compensated donor photoconductor should result in a large positive temperature coefficient of photocurrent over the temperature range in which the probability of thermal ionization of holes bound to the low-lying compensating acceptor impurity goes from a low to a high value. Curves giving the temperature dependence of  $\Delta\sigma_g$  per watt of black body radiation, chopped at 100 cps, from a source at about 300°K, for three different gold doped samples, are shown in Fig. 21. The concentrations of gold and gallium, the values of  $\Delta\sigma_g$  at 5°K and the ratios of  $\Delta\sigma_g$  at 13°K to those at 5°K are given in Table VI for these samples.

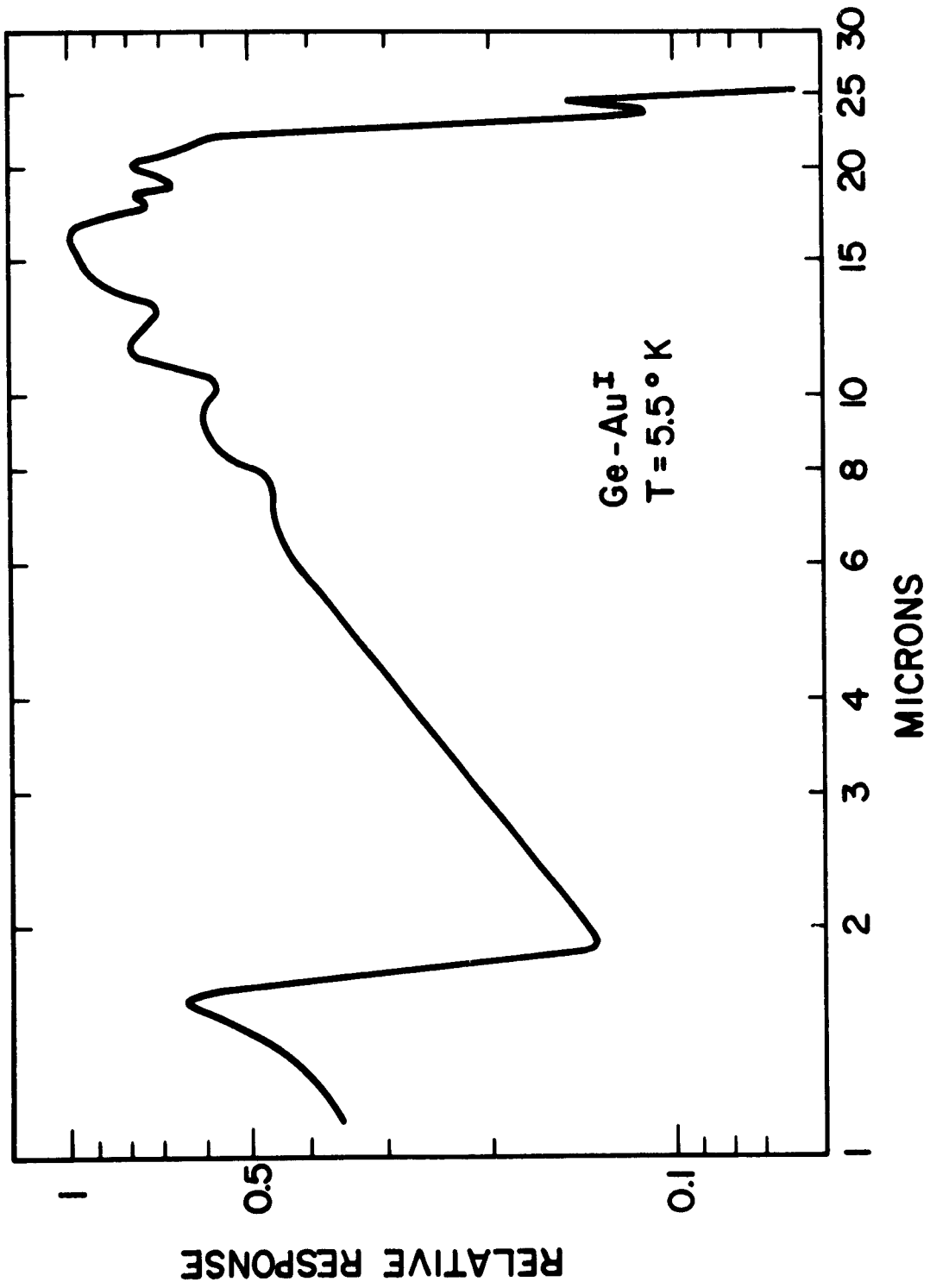


FIG. 20

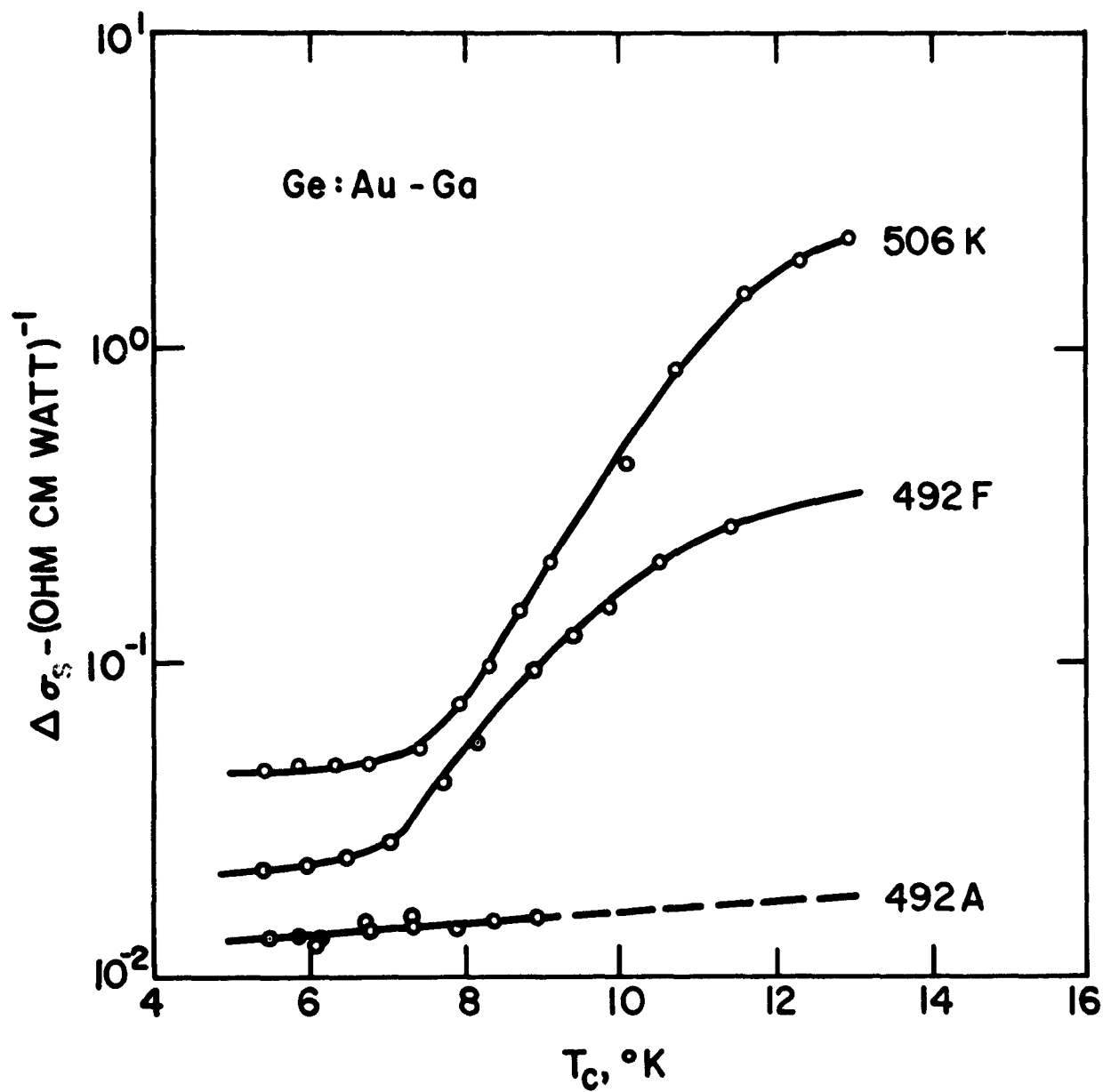


FIG. 21

TABLE VI Ge-Au <sup>I</sup> - Temperature Dependence of Photocurrent				
Sample	Photocurrent Ratio (13°K/5°K)	$\Delta\sigma_g$ at 5°K (ohm cm watt) <sup>-1</sup>	Total Gold Conc. cm <sup>-3</sup>	Gallium Conc. cm <sup>-3</sup>
506K	52	$4.4 \times 10^{-2}$	$2.2 \times 10^{14}$	$1.9 \times 10^{14}$
492F	14	$2.2 \times 10^{-2}$	$6.3 \times 10^{14}$	$5.7 \times 10^{14}$
492A	1.4	$1.3 \times 10^{-2}$	$6.4 \times 10^{14}$	$3.4 \times 10^{14}$

The differences in behavior are striking. The photocurrent ratio is about unity for 492A and in excess of fifty for 506K. The question of whether or not these results provide evidence for a small capture cross section for the gold recombination centers will now be examined. At a high temperature, e.g., 13°K, only the gold recombination centers are operative. Their concentration is the difference between the gold and the gallium concentrations. At a low temperature, e.g., 5°K, two hypotheses will be considered.

- (a) The gold cross section is negligible compared with that of gallium.

The concentration of recombination centers for this case is  $(G_a - \Delta)$  where  $G_a$  is the total gallium concentration and  $\Delta$  is the concentration of gallium centers containing bound holes due to the redistribution under the influence of background radiation.

- (b) The gold and gallium have equal cross sections. The recombination center concentration for this case would be equal to the total gold concentration. The various recombination center concentrations are listed in Table VII.

Sample	Low Temperature		High Temperature
	(a)	(b)	
506K	$1.9 \times 10^{14} - \Delta_1$	$2.2 \times 10^{14}$	$3 \times 10^{13}$
492F	$5.7 \times 10^{14} - \Delta_2$	$6.3 \times 10^{14}$	$6 \times 10^{13}$
492A	$3.4 \times 10^{14} - \Delta_3$	$6.4 \times 10^{14}$	$3.0 \times 10^{14}$

Consider first the  $\Delta\sigma_g$  values at 5°K. The experimental values are inconsistent with hypothesis (b) since this would require that samples 492A and 492F have the same value of  $\Delta\sigma_g$  while sample 506K should have a value 2.9 times larger. Hypothesis (a) cannot reliably be checked since the values of the  $\Delta$ 's cannot be determined without a knowledge of the cross section ratio B.

A definite conclusion may be drawn from the relative values of  $\Delta\sigma_g$ , at the high temperature since here only the gold recombination centers are involved. From the concentrations given in Table VII and assuming that the gold center cross section is the same in all three samples, the  $\Delta\sigma_g$  ratios expected at 13°K are:  $\frac{506K}{492F} = 2$ ,  $\frac{506K}{492A} = 10$ , and  $\frac{492F}{492A} = 5$ . The experimentally observed values are 7.4, 126, and 16.9, respectively. The assumption of a constant cross section for the gold center is clearly inconsistent with the results. The magnitude of the cross section must be a function of the gold and gallium concentrations. The data, at present, are not sufficiently complete to determine the form of this functional dependence.

Considering the change of  $\Delta\sigma_g$  with temperature for each sample individually, hypothesis (b) requires that the photocurrent ratios be 7.3, 10, and 2.1 for samples 506K, 492F, and 492A, respectively, provided that the cross sections

are temperature independent. If the cross sections are assumed to be temperature dependent with the same sign of temperature coefficient as has been reported for other impurities (cross section increases with increasing temperature), then the expected ratios would be even smaller than these. Except possibly for sample 492A, the observed ratios are substantially larger. This argument suggests that the capture cross section for the gold level is considerably smaller than that for gallium which may be taken as being representative of a normal acceptor impurity. It is not possible to make a reliable comparison with experiment on the basis of hypothesis (a) since, once again, the  $\Delta$ 's cannot be evaluated without a knowledge of the cross section ratio B at the low temperature. Even if this quantity were known, it would be difficult to estimate the expected increase of photocurrent with temperature without a knowledge of the temperature and concentration dependence of the gold cross section.

The one point which appears to have been rather definitely established from the results thus far obtained is that the gold center recombination cross section appears to be concentration dependent. The results suggest, but do not definitely establish, that the gold cross section is significantly smaller than the gallium. Clearly, more experimental work is required. Of prime importance is the more accurate determination, by Hall effect measurements, of impurity concentrations. Knowledge of carrier mobilities in the high temperature range where recombination with gallium is not involved should permit the determination of lifetimes and therefore capture cross sections from measurements of photocurrents excited by known photon fluxes. If the cross sections can be obtained as a function of temperature in the high temperature range, then, by extrapolation, low temperature values can be estimated and compared with experimentally determined values in order to obtain cross sections for gallium.